https://www.overleaf.com/18650500wbzfjbmyrv

INVESTIGATION OF THE EFFECTS OF NF-κB ON OTA INDUCED APOPTOSIS IN HK-2 CELL LINE

by

Can Gürkaşlar

B.S., Molecular Biology and Genetics, Istanbul Technical University, 2015

Submitted to the Institute for Graduate Studies in
Science and Engineering in partial fulfillment of
the requirements for the degree of
Master of Science

Graduate Program in Molecular Biology and Genetic

Boğaziçi University

2018

ACKNOWLEDGEMENTS

First, I would like to thank my supervisor Assoc. Prof. Ibrahim Yaman for letting me to work in his laboratory, for his guidance and mentorship throughout my Master's studies.

I also thank my jury members Assist. Prof. Necla Birgül and Assoc. Prof. Ferruh Ozcan for spending their valuable time by evaluating my thesis.

I'm grateful to former and current members of MTCRL; Hazal Zırhlıoğlu, Ayşin Akpınar, Beren Aylan, Ahmet Aktaş, Gizem Gül and Onur Kerem Tever for their hands-on help during my experiments and their friendship outside the laboratory.

I would like to give special thanks to our sister lab members, Aybüke Garipcan, Mesut Berber, Açelya Yılmazer, İlke Süder, Gizem Olay Artık, Orhun Külekçi for precious memories and support throughout this study.

I am also very pleased to meet former and current GEBİT members; Altuğ Didikoğlu, Bilal Başdağ, Elif Bozlak, İbrahim Taşkıran, Harun Öztürk, Uğurcan Sakızlı, Emir Erkol, Selif Eski for creating inconceivably sincere habitat in recent years.

Words can't describe how helpful Mr.Argör Mehmet Can Demirler was when he had excused me from cleaning duty.

Finally, my deepest gratitude goes to my family, Hasan and Serap Gürkaşlar for their love and unconditional support since forever. Without their support I would not be able to complete my thesis. My special thanks goes to Kübra Zırhlıoğlu for her guidance, help and encouragement in my experiments and during the process of writing this thesis.

ABSTRACT

INVESTIGATION OF THE EFFECTS OF NF-κB ON OTA INDUCED APOPTOSIS IN HK-2 CELL LINE

Ocharoxin A (OTA) is a mycotoxin produced by certain species of *Aspergillus* and *Penicillium* genera of fungi. OTA was shown to be carcinogenic, genotoxic, immunotoxic by many studies and main suspected causative agent for Balkan Endemic Nephropathy. OTA induces oxidative stress, causes cell cycle arrest and deregulates various signaling pathways. There is no study relating the NFκB activity and apoptosis upon OTA treatment. In this study, we have shown that OTA induces canonical NF-κB pathway in HK-2 cells. OTA mediates nuclear translocation of p65 subunit of NF-κB as well as NF-κB-driven gene expression. Moreover, We observed that, when NF-κB pathway was inhibited by Bay11-7085 OTA-induced Erk1-2 phosphorylation was diminished. Our results suggest that NF-κB inhibition also abate Erk1-2 mediated apoptosis upon OTA treatment. Finally, we have generated K310R-RelA HK-2 cell line expressing dominant-negative form of p65 subunit of NF-κB. Prolonged OTA exposure of these cells decreased Erk1-2 phosphorylation compared to control cells. However, the suppression of OTA-induced apoptotic cell death observed with chemical inhibition of NF-κB could not be achieved with this stable cell line. In conclusion, our results shed light on another major pathway affected by OTA and disclose one of the missing steps in OTA mode of action and relate it with foreknown effects of OTA, Erk1-2 phosphorylation and induction of apoptosis.

ÖZET

OKRATOKSİN A GÜDÜMLÜ APOPTOZDA NF-B'NİN ETKİLERİNİN HK-2 HÜCRE HATTINDA İNCELENMESİ

Okratoksin A (OTA) mantarların *Aspergillus* ve *Penicillium* cinsinin belirli türleri tarafından üretilen bir mikotoksindir. OTA'nın karsinojenik, genotoksik ve immünotoksik etkileri birçok çalışma ile gösterilmiştir ve Balkan Endemik Nefropatinin ana sebeplerinden biri olduğu düşünülmektedir. OTA'nın oksidatif strese neden olmak, hücre bölünme döngüsünü durdurmak ve çeşitli sinyal yolaklarını bozmak gibi etkileri vardır. Şu ana kadar OTA kaynaklı NF-κB aktivitesi ile apoptozu ilişkilendiren bir çalışma mevcut değildir. Mevcut projede OTA'nın HK-2 hücrelerinde standart NF-κB yolağının aktive olmasına neden olduğu gösterilmiştir. OTA p65'in çekirdeğe geçisini ve p65 tarafından ifade ettirilen genlerin translasyonunu arttırmaktadır. Buna ek olarak NF-κB yolağı inhibitörü olan Bay11-7085'in OTA ile birlikte verildiğinde OTA tarafından arttırılmakta olan Erk1-2 fosforilasyonunu azaltmaktadır. Sonuçlarımız Erk1-2 aracılığı ile aktive olan apoptozun da Bay11-7085 verildiğinde azaldığını göster- mektedir. Son olarak dominant-negatif etkiye sahip K310R-RelA mutant proteinini sürekli bir şekilde ifade eden HK-2 hücre hattı üretilmiştir. Bu hücrelere uzun süreli OTA muamelesinde Erk1-2 fosforilasyonunun kontrol hücrelerine oranla azaldığı göz- lemlenmiştir. Ancak, apoptotik hücre ölümünü engellemede etkisi sınırlı kalmıştır. Özet olarak sonuçlarımız OTA tarafından etkilenen bir sinyal yolağını daha ortaya çıkarmış ve OTA'nın etki mekanizmasında bilinmeyen bir basamağa daha ışık tutmuştur ve önceden bilinmekte olan Erk1-2 fosforilasyonu ve apoptoz ile bağlatı kurulmuştur.

TABLE OF CONTENTS

LIST OF FIGURES

LIST OF TABLES

LIST OF SYMBOLS

g	Gram
h	Hour
kDa	Kilodalton
L	Liter
M	Molar
mg	Miligram
ml	Mililiter
mm	Milimeter
mM	Milimolar
ng	Nanogram
V	Volt
α	Alpha
β	Beta
δ	Delta
κ	Kappa
μg	Microgram
μl	Microliter
μM	Micromolar
^{o}C	Degree Celcius

LIST OF ACRONYMS/ABBREVIATIONS

AP	Alkaline Phosphatase
APS	Ammonium Persulfate
ATG	Autophagy Related Protein
BEN	Balkan Endemic Nephropathy
BSA	Bovine Serum Albumin
DAPI	4',6-Diamidino-2-Phenylindole
DMEM	Dulbecco's Modified Eagle's Media
DMSO	Dimethyl sulfoxide
DNA	Deoxyribonucleic Acid
ERK1-2	Extracellular Signal-Regulated Kinase 1-2
EtOH	Ethanol
FBS	Fatal Bovine Serum
GFP	Green Fluorescence Protein
HBS	HEPES Buffer Saline
HK-2	Human Kidney 2
HRP	Horseradish Peroxidase
IKBα	nuclear factor of kappa light polypeptide gene enhancer in B-cells inhibitor, alpha
MAPK	Mitogen Activated Protein Kinase
MEK	Mitogen-activated Protein Kinase Kinase
NaCl	Sodium Chloride
NF-κB	Nuclear factor kappa B
OTA	Ochratoxin A
PBS	Phosphate Buffer Saline
PCR	Polymerase Chain Reaction
PFA	Paraformaldehyde
PI3K/AKT	Phosphoinositide 3-kinase/Protein Kinase B
PVDF	Polyvinylidene fluoride

RNA	Ribonucleic Acid
ROS	Reactive Oxygen Species
RT	Room Temperature
SDS	Sodium Dodecyl Sulfate
sgRNA	Single Guide RNA
TBS-T	Tris Buffer Saline-Tween 20
TEMED	Tetramethylethylenediamine
VHC	Vehicle
XTT	sodium 3´-[1- (phenylaminocarbonyl)-3,4-tetrazolium]-bis(4-methoxy-6-nitro

1. INTRODUCTION

Mycotoxins as food contaminants have been widely studied since they are known to cause various diseases, especially cancer. Mycotoxins are secondary metabolites produced by fungi and classified as abiotic hazards due to their risks when being eaten, breathed or in skin contact. Mycotoxins enter food chain through fungi contaminated foods and feeds that are directly consumed by humans and animals. After digestion, mycotoxins can accumulate in different organs or tissues [1].

Ochratoxin A (OTA) is a mycotoxin mainly produced by fungal species *Penicillium verrucosum, Aspergillus ochraceus* and *Aspergillus carbonarius* . OTA can contaminate wide range of foods like grapes, wine, grain products, legumes, coffee, cacao, spices, dried fruits etc. Moreover, OTA contaminated animal feed causes OTA to accumulate in blood serum, kidney and liver of animals [2]. Similarly medicinal plants and herbal teas were reported to be contaminated with OTA. Between 50-100% of the tested human blood serums, kidneys and human milk were found to contain OTA [3]. Although found in trace amounts, with its high stability and wide range food contamination, humankind continuously exposed to OTA [2].

OTA was shown to increase kidney adenoma and carcinoma in rats and male mice. Moreover, it was found to increase liver tumor growth in mice [4, 5]. In humans, it's thought to be associated with Balkan Endemic Nephropathy (BEN) and urinary system tumors [6]. Based on the animal studies showing nephropathic, nephrocarcinogenic and immunotoxic effects of OTA , International Agency for Research on Cancer (IARC) announced OTA as a possible human carcinogen type 2B [5].

There are different proposed models on how OTA elicits its carcinogenicity. In one hand, it is proposed that OTA and/or its metabolites are genotoxic and binds DNA covalently, thereby, promoting carcinogenesis. On the other hand, it has been proposed that OTA shows its carcinogenic effect by epigenetic mechanisms to trigger

tumor formation as a non-genotoxic carcinogen [7–10]. Among epigenetic mechanisms DNA damage caused by oxidative stress, mitochondrial function abnormalities, evasion of apoptosis, inhibition of macromolecule synthesis and reprogramming of signal transduction pathways have been proposed [11–15]. Despite intense studies, OTA's mode of action in carcinogenesis yet to be discovered.

1.1. Ochrotoxin A (OTA)

OTA was first isolated in 1965 from *Aspergillus ochraceus* Wilh and defined as a toxic metabolite. In the same year, ochratoxin B (OTB) and ochratoxin C (OTC), analogs of OTA, were also discovered. OTA consists of L-β-phenylalanine group connected to a dihydroisocoumarin (7-carboxy-5-chloro-8-hydroxy-3,4-dihydro-3R-methylisocoumarin) molecule with a peptide bond. OTA is the most toxic form amongst all forms of ochratoxins. Hydrolysis of OTA results in Ochratoxin α and phenylalanine [16]. Chemical structure of OTA and its resulting metabolites shown in Figure 1.2. Ochratoxin α is a dihydroisocoumarin molecule with chlorine molecule and it is the most common OTA metabolite in all species tested [17].

OTA is an highly stable molecule, therefore, known food processing techniques are not able to degrade OTA. It was reported that 250°C for 6 minutes needed for degradation of 50% of OTA [18]. Besides, 3R-epimers of OTA which was induced with heat was detected. Roasted coffee and human blood serum also has 3S-epimer of OTA [19]. Biological half-life of OTA differ from species to species where 42 minutes in fish , 510 hours in monkeys and 840 hours in human,based on one volunteer male [20].

1.1.1. Absorbtion, Metabolism and Excretion of OTA

As a weak organic acid, OTA's pKa varies between 4.2 and 7.3 owing to carboxyl and phenolic groups present in its structure, respectively. This acidic residues mediates absorption of OTA [21]. Full form of OTA has lipophilic character while hydrolized forms have hydrophilic properties [22].

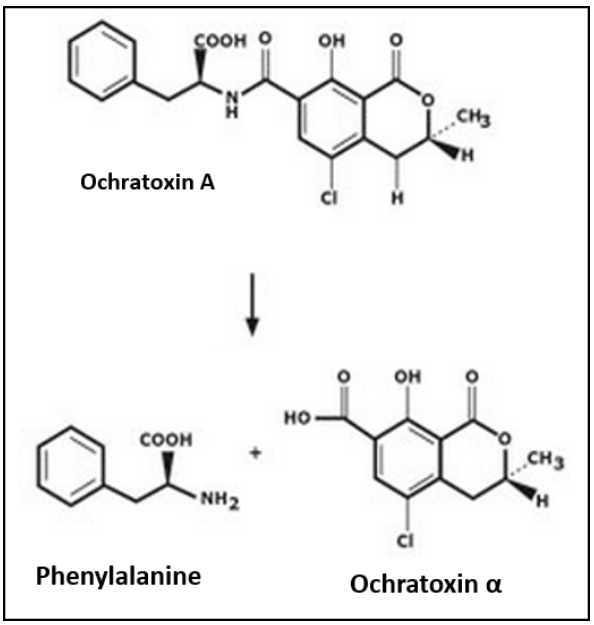

Figure 1.1. Chemical structure of OTA and its hydrolysis products (Adopted from Altiokka *et.al.*, 2009)

OTA is absorbed through all gastro-intestinal track but mainly on small intestine and carried to the kidneys. Ninety-nine percent of OTA binds to serum proteins especially albumin. By this way, its biological half-life in humans is extended. While the organic anion transporter (OAT) proteins facilitate the disposal of OTA from kidney tubules, again OAT and H^+-dipeptide transporter proteins help re-absorbtion of OTA back to nephron tubules [23]. These transporters cause accumulation of OTA in kidneys [24]. Therefore, kidney is thought to be the main target organ for OTA, although, its presence was shown in liver, muscles and fat tissues as well [17].

1.1.2. Toxicity of OTA

A study by National Institutes of Health, National Toxicology Program demonstrated that OTA is a nephrotoxic substance and a renal carcinogen in rats [25]. Later, it was shown that even smallest concentrations of OTA can induce kidney tumors in rats [26]. It has been reported that male mice is more susceptible to OTA, however, the presence of breast fibroadenoma in female mice was detected as well [26, 27].

Due to kidney being the primary target, nephropathy and urinary system cancers were linked to OTA. In animals, it has also been shown that OTA intake was directly correlated with testicle cancer. Moreover, teratogenic, genotoxic, carcinogenic and immunotoxic effects of OTA were suggested based on other animal studies [1].

In vitro experiments with Vero [28], NRK-52ELLC-PK1 [29], V79 [30], OK cell lines and primary cell cultures [31] strongly indicates that OTA is a cytotoxic agent and results in triggering proliferative responses .

1.1.3. Possible Mechanisms Mediating OTA Toxicity

In literature, the mechanisms that have been proposed to explain direct or indirect OTA-mediated toxicity are; inhibition of macro-molecule synthesis, DNA adduct formation, lipid peroxidation, oxidative damage and mitochondrial dysfunction [22].

The gross effects of OTA on animals have been widely studied. On the other hand, to understand the effects at the cellular and molecular levels, cell culture studies are beneficial. Studies using cell lines from different species, primary cell cultures illustrate that response to OTA varies among different cell types; while some cells are resistant to OTA toxicity, some others are affected by much lower concentrations of OTA.

1.1.3.1. Inhibition of Macromolecule Synthesis. OTA contains phenylalenine amino acid (Phe) in its chemical structure. Hence, it has been thought that OTA inhibits many enzymes that use phenylalenine as a substrate. It was suggested that OTA can hinder protein synthesis by inhibiting Phe-tRNA synthetase. OTA was shown to inhibit purified *Bacillus subtlis* Phe-tRNA synthetase enzyme *in vitro* [32].

1.1.3.2. Oxidative Stress. Aerobic organism need oxygen to survive. Oxygen tend to form reactive oxygen species (ROS) like hydroxyl ions and superoxide. In homeostasis, ROS production and neutralization is in balance, therefore, oxidative stress will not

occur. External factors, however, can derange the balance and cause oxidative stress, which could damage vital cellular parts and put cell vitality in danger. Accumulation of ROS causes inevitable oxidation of lipids, proteins and nucleic acids [33]. Increments in oxidative stress can cause pathological conditions like cancer, neurodegenerative diseases and aging [34].

1.1.3.3. DNA Adduct Formation. Pfohl-Leszkowicz and her colleagues proposed that OTA and/or its metabolites are directly binding to DNA by covalent bonds, therefore, it is genotoxic. They used ^{32}P-labelling method to visualize DNA adducts. According to their study, OTA treatment caused DNA adduct formations in both kidney and liver in mice and rats. These adducts can be subsided in the presence of anti-oxidants by 90% [35]. Another study used tritium labelled OTA and ^{32}P-labelling method combined and could not detect adduct formation and concluded that DNA damages are the result of increased ROS rather than OTA itself [36].

1.1.3.4. Apoptosis. Apoptosis, known as programmed cell death, is an evolutionary conserved death mechanism that has role in various biological systems from development to immune system progression [37]. First, cells shrink then cell nucleus is condensed, and then cell breaks apart in pieces enclosed by membrane. Activation of caspase protein family, PARP (poly ADP-Ribose Polymerase) cleavage and DNA fragmentation are distinct markers for apoptosis [38].

Caspase 3 and caspase 7 are known as effector caspases and essential regulators of apoptosis. They regulate mitochondrial events, mitochondrial membrane potential($\Delta\psi$m), release of apoptosis inducing factor(AIF). Moreover, they amplify initiation signal and promote upcoming cytochrome c release. It has been shown that fragments of caspase 3 arrange morphological changes, caspase 7 has less role in this process. Role of caspase 7 in apoptosis is more focused on regulating loss of cell viability. Cleavage of PARP is also dependent on caspases 3/7 [39].

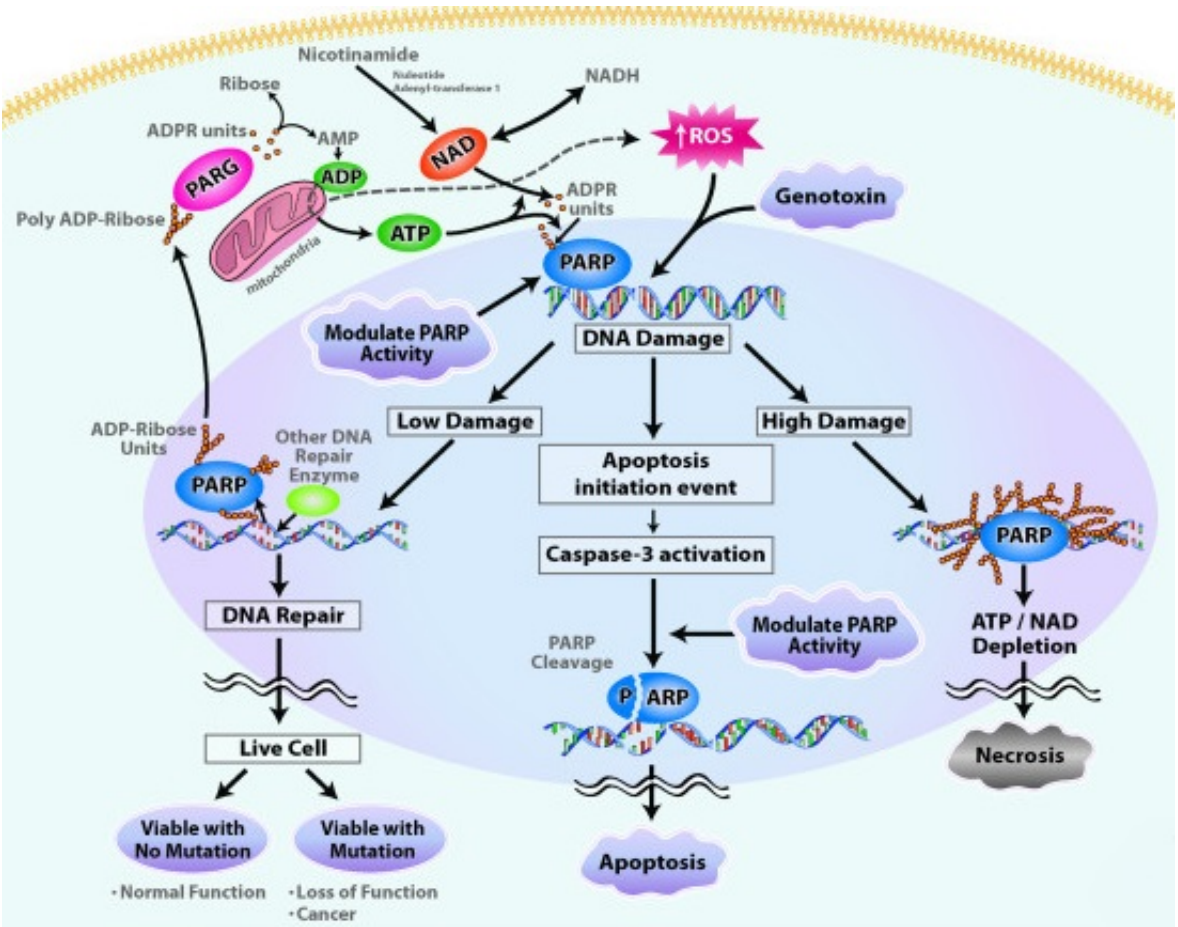

Figure 1.2. Mechanism of apoptosis induction (Adopted from Agarwal *et al.*, 2009)

Nuclear protein PARP (116 kDa) specifically cleaved during apoptosis resulting 85 kDa fragment [37]. PARP protein recognizes DNA breaks and gets activated, uses NAD^+ molecule as a donor and form ADP-ribose polymer. Ester bonds on this polymer added on positively charged amino acids in target proteins which is known as PARylation. Over-activation of PARP in damaged tissue is correlated with mitochondria-associated cell dead [40]. Lühe *et al.* have shown that OTA causes upregulation of some genes belonging apoptotic pathway both in *in vivo* and *in vitro* conditions via microarray analysis (Figure 1.2) [41].

A study on rats also showed that OTA causes a significant increase in apoptotic cell count from distal and proximal tubular cells in kidneys by using TUNEL (Terminal

deoxynucleotidyl transferase mediated dUTP Nick End Labeling) method. When rats were fed with OTA contaminated food, the number of apoptotic cells were increased by five-fold after 10 days, 6.4-fold after 30 days and 12.7-fold after 60 days [12].

1.1.3.5. Effects of OTA on Immunity and Cellular Immune Response. OTA is known for its cytotoxic and carcinogenic effects. Some studies have also shown the immunotoxic effects of OTA. It is not conspicuous whether OTA directly causes immunotoxicity or its acute toxicity leads immunotoxicity. Nevertheless, much lower concentrations than acute toxicity have been shown to induce immunotoxic effects [42] in mouse model.

Animal studies conducted by different groups have shown immune suppression in various cell types of immune system by OTA. Low IgG titers in chicks [43], BALB/c mice [44] indicated T-cell inhibition. Lea *et al.* have shown B-lymphocyte inability to synthesize antibody independent from T-cell inhibition [45]. Moreover natural killer (NK) cells were also affected by OTA lowering the interferon secretion in mice [46]. Besides, OTA can induce pro-inflammatory cytokines IL-6 and IL-8 even from nasal epithelial cells [47].

1.2. Mitogen-Activated Protein Kinases(MAPKs)

External stimuli received from extracellular signals are perceived and amplified by MAPKs which could combine multiple signals. Signals that are transduced via MAPKs lead to changes either by promoting transcription or physically interacting with other proteins depending on environmental fluctuations [48]. MAPK pathways are three-tiered kinase cascades; MAPKKKs (MAPK kinase kinases), MAPKKs (MAPK kinases), and MAPKs [49]. MAPKs consist of four conventional families, ERK1/2, p38, c-Jun N-terminal Kinase(JNK) and ERK5, first three being the most studied ones. Non-conventional ones are ERK3/4, ERK7/8 and Nemo-like Kinase(NLK) [50].

For tumorogenesis, six critical parameters have to be altered; cell proliferation independent of extra/intracellular signalling, ability to escape apoptosis, reduced ef-

fectiveness of growth suppressors, spreading, ability to generate extra veins vessels for increased nutritional needs and finally metastasis [51].

1.2.1. MEK/ERK Signalling Pathway

Activated Raf (which is a MAPKKK) phosphorylates MEK1 and MEK2 from their specific serine residues and activates them. Three different isoform of Raf are responsible for MEK1/2 phosphorylation. B-Raf is the most prominent kinase, A-Raf is rather weak kinase and only activates MEK1. c-Raf uniformly phosphorylate MEK1 and MEK2. Activated ERKs (Extracellular-signal Regulated Kinases) phoshphorylate various targets having roles in proliferation, migration, angiogenesis, survival, chromatin remodelling and apoptosis depending on cell type and stimuli [49].

Prolonged activation of ERK regulates cyclin D1 which has role in cell cycle, moreover, it represses the activity of genes inhibiting cell proliferation [52]. Contrarily, Mirza *et al.,* have shown robust ERK activation breaks the cell cycle [53]. Apoptotic role of ERK1-2 signal is being discovered by recent studies. Notably, apoptotic renal and neuronal cell deaths were linked to ERK1/2 activation under different stress conditions and toxic substances [54–56]. Moreover, our group has shown that apoptotic cell death caused by OTA can be mitigated by MEK1/2 inhibitor U0126 [57].

1.3. NF-κB Family and Their Roles in Cellular Signalling

NF-κB transcription factors are elements in cell signalling in response to external or physiological stimuli which is essential for keeping the homeostasis of cells. These various stimuli activates NF-κB family and eventually will lead to activation of major cellular responses like immune response, apoptosis, proliferation, survival, stress response and differentiation [58]. NF-κB family consists of five members. As Figure 1.3 demonstrates, they all contain N-terminal Rel-homology domain (RHD) which enables them to make homo/heterodimers, bind to DNA and localize to the nucleus. This domain also helps the binding of inhibitory proteins. RelA, RelB and c-Rel have C-

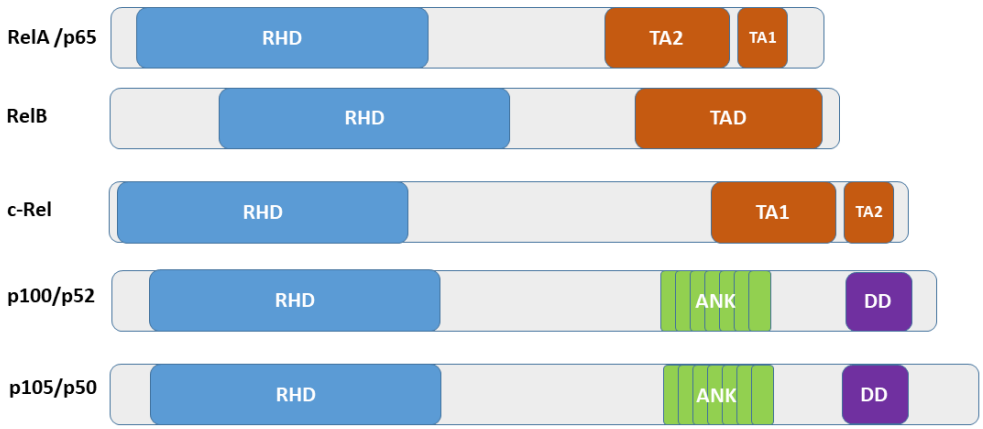

Figure 1.3. Five members of NF-κB family; RelA(p65), RelB, c-Rel, p100/p52 and p105/p50 and domains they contain

terminal transcriptional activation domains (TADs). In RelA and c-Rel, TAD consists of two subdomains. In spite of having resembling structure, these TA domains have different and non-overlapping functions [59]. Ankyrin repeats found in p105 and p100 are also found in inhibitor of κB (IκB) family which has a role inhibiting NFκB dimers that they interact with [60].

NF-κB proteins are considered to be rapid response transcription factors. When external signal is absent, they are mostly found in cytoplasm paired with Inhibitor κB (IκB) family (IκBα, IκBβ, IκBϵ) proteins in inactive state or as a precursor forms of NFKB1 and NFKB2(p105 and p100, respectively). When activating stimuli received, IκB proteins are phosphorylated by upstream IKKα/β kinases from their conserved residues. IκB proteins have DS*GXXS* consensus motif where serines can be phosphoylated. This motif allows Skp1-Culin-Roc1/Rbx1/ Hrt-1-F-box (SCF) E3 ubiquitin ligase complexes ($SCF^{\beta TrCP}$) and E2 of Ubc4/5 family bind and ubiquitinylate IκB proteins [61]; eventually leads to proteosomal degradation and exposure of nuclear localization signal (NLS) of NF-κB proteins [62] and nuclear translocation(Figure 1.4).

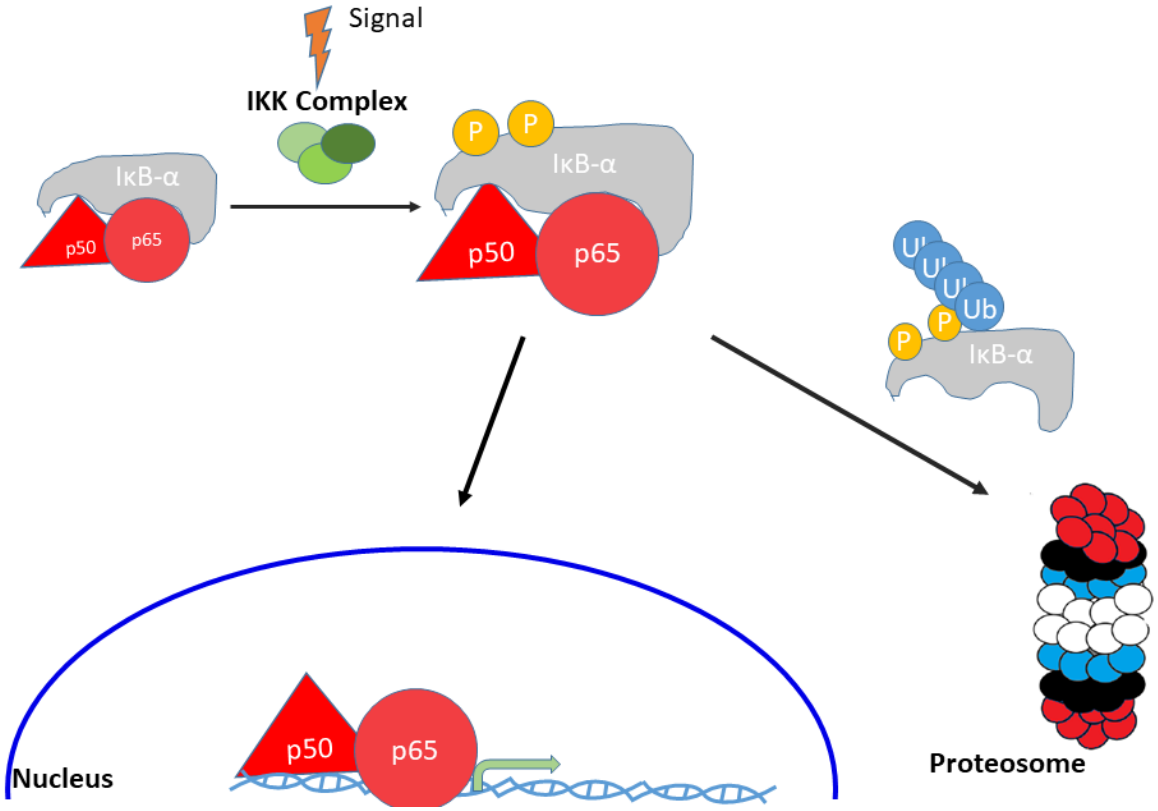

Figure 1.4. Representation of canonical NF-κB pathway activation and nuclear translocation(Adopted from Tabruyn S.T. *et.al.*, 2008).

1.3.1. Post-translational Regulations of NF-κB

Given the massive number of genes regulated by NF-κB proteins and small number (only five) of subunits forming a functional NF-κB, different layers of regulation is expected. Different homo/hetero-dimerizations, recruitment of additional transcription factors and co-activators, regulation of histone tails near promoter regions in the NF-κB target genes [63] are the well-known different layers of regulation. Post-translational modifications (PTM) is another layer for this purpose. p65 (RelA) is the most studied NF-κB family proteins and has been shown to be a target of many PTM sites.

1.3.1.1. Phosphorylation of p65. p65 has seven serines and three threonines that were shown to be phosphorylated and dephosphorylated by different kinases and phospho-

tases, respectively [64]. S276 phosphorylation is the first discovered one. PKAc or MSK-1 are kinases responsible for this phosphorylation. Phosphorylation lessen the interaction between N- and C- termini and favors the binding of p300/CBP co-activator proteins which also has acetyl-transferase property [65]. On the whole, S276 phosphorylation enhances its transcriptional activation [66].

S536 phosphorylation is done by IKKs, RSK1 and TBK-1 kinases [67–70] in response to different stimuli. S536 phosphorylation also increases transcriptional activity by enhancing affinity for p300 and reducing the binding to SMRT (a co-repressor) [71, 72]. S468 phosphorylation is done by GSK3β, IKKβ and IKKε kinases. Binding of COMMD1-containing E3 ligase complex is promoted, ubiquitynation causes degradation of p65 thereby decreasing its transcriptional activity [68, 73].

Other phosphorylation sites S205, S281, S311, S529, T254, T435 and T505 were relatively less studied and certain details of their phosphorylation mechanisms still remain unclear. In short; S205 and S281 phosphorylations were shown to be activated by LPS treatment affecting transcription of target genes [74]. S311 has comparable mode of action with S276 and S536 by recruiting p300 and increasing transcriptional activity [75]. T435 and T505 phosphorylations have negative effect on p65 activity on target genes [76, 77].

1.3.1.2. Acetylation of p65. Seven lysine residues (K122, K123, K218, K221, K310, K314 and K315) were found to be acetylated mostly by p300/CBP complex and sometimes PCAF [78]. Acetylations on K218 and K221 increase DNA binding ability of p65. In addition, K218 acetylation hinders IκB binding sites thereby inhibiting nuclear export of p65 [79]. K122 and K123 acetylation were shown to inhibit p65 to bind κB binding site [80]. Buerki *et al.,* have shown that K314 and K315 acetylation does not seem to affect p65 conformation, however, affects transcription of specific sets of genes upon TNF-α stimulation [81].

Chen *et al.,* claimed that K310 acetylation does not affect DNA binding ability and proved by showing acetylation deficient K310R mutant p65's ability to bind DNA probe in electrophoretic mobility shift assay(EMSA). However, inability to get acetylated by p300/CBP sharply decreased NF-κB-dependent gene expression shown by luciferase assay [79].

1.3.1.3. Methylation of p65. Set9 is the methyltransferase that is responsible most of the methylation on p65. K314 and K315 are methylated by Set9 and result in ubiquitylation and degredation [82]. On the other hand, methylation on K37 results in activation/repression of specific subset of NF-κB target genes [83].

1.3.2. NF-κB in Apoptosis

Earlier in the discovery of NF-κB, it was thought that NF-κB is an antiapoptotic protein, however, later studies found that in some cases it can drive cells to programmed cell death(PCD). p65 stands in the middle of the cross-roads, determining the cell fate.

Canonical pathway starts with binding of TNF-α to TNFR. This can initiate multiple downstream pathways depending on adaptor proteins recruited to the cell membrane. One of them is binding of TNFR-associated Death Domain (TRADD) to TNFR followed by recruitment of RIP1 and TNFR-associated factor 2 (TRAF2). IKK is phosphorylated by this complex leading NF-κB activation and expression of anti-apoptotic proteins, like FLICE/caspase8 inhibitor protein (c-FLIP). c-FLIP inhibits the activity of caspase 8 which is another survival pathway activated by TNFR/TRADD complex protecting the cell from apoptotic route [84]. Other TNFR-downstream pathway starts with RIP1 recruitment to TNFR without TRADDs presence. RIP1 increases ROS production and activates JNK cascade [85] and from there cells undergo apoptosis or necrosis determined by cells metabolic state, however, the mechanism is still unclear [86].

Although generally accepted as a survival factor, in some cases NF-κB acts as a

proapoptotic factor. Kirsteen *et al.,* have shown that UV-C treatment and some chemical reagents increased NF-κB activation while decreased the mRNAs of NF-κB target antiapoptotic genes like Bcl-xL, X-IAP, and A20 [87], which illustrates the proapoptotic side of NF-κB. Moreover, the expressions of proapoptotic genes like Fas [88], FasL [89], DR4 and DR5 [90] are also controlled by NF-κB.

2. HYPOTHESIS AND PURPOSE

Because OTA is a mycotoxin found in human food and animal feed, continuous exposure results in various dysregulations at the organismal and cellular levels that were described in the introduction section. Nonetheless, the mode of action(s) for OTA cytotoxicity and carcinogenicity are not fully elucidated. In addition, OTA is also known for its immunotoxic properties [43, 45, 46], improper NF-κB activation is an important indicator of immunotoxicity and, in fact, some groups have shown phosphorylation and translocation of NF-κB to the nucleus during immune cell toxicity induced by OTA [91–93]. However, there are no study relating NF-κB activation to OTA-induced apoptosis since NF-κB is generally known as pro-survival factor. Nevertheless, recent studies have demonstrated that some chemical agents display pro-death properties through NF-κB activation as mentioned in section 1.3.2.

We hypothesized that OTA may cause improper NF-κB activation and apoptotic cell death during the treatment. Furthermore, we expected inhibition of NF-κB could reduce or abolish the apoptotic cell death upon OTA treatment. In order to verify our hypothesis following aims were established.

- *in vitro* investigation of the effects of OTA on NFκB pathway activation in HK-2 human kidney proximal tubular epithelial cells.

- *in vitro* investigation of relationship between NF-κB and other OTA-induced signaling pathways

- Examining the effects of NF-κB inhibition on apoptosis.

3. MATERIALS

3.1. Cell Culture

Unless it is documented otherwise in the tables, all of the chemicals and cell culture reagents were ordered from Sigma-Aldrich (USA) and Gibco, Fisher Scientific (USA), respectively. All disposable plasticwares were ordered from TPP (Switzerland) and CAPP (Denmark).

Table 3.1: Cell Culture Solutions.

DMSO	Sigma-Aldrich, USA
Dulbecco's Modified Eagle's Medium/Nutrient F-12 Ham	PAN, Germany
Fetal Bovine Serum (FBS)	Gibco, Fisher Scientic, USA
Lipofectamine 2000	Invitrogen, USA
Opti-MEM	Gibco, Fisher Scientic, USA
Penicillin/Streptomycin (100X)	Gibco, Fisher Scientic, USA
Trypsin-EDTA (0.5 mM EDTA, 0.025% Trypsin)	Gibco, Fisher Scientic, USA

Table 3.2: Cell Lines.

Cell Line	**Provider**
Human Kidney 2 (HK-2) Cells	ATCC #CRL2190
K310R-RelA Human Kidney 2 Stable Cells	MTCRL- Obtained from ATCC #CRL2190 by K310R-RelA Stable Transduction

Table 3.2. Cell Lines (cont.).

Cell Line	**Provider**
GFP-RelA Human Kidney 2 Stable cells	MTCRL-Obtained from ATCC #CRL2190 by GFP-RelA Stable Transduction
HeLa Cells	Kindly provided by Cemalettin Bekpen, PhD, Max Planck Institute for Evolutionary Biology

3.2. Plasmids and Primers

Plasmids T7-RelA-K310R (no:23250) and GFP-RelA (no:23255) were ordered from Addgene. psPAX2 lentiviral packaging vector, pCMV-VSV-G lentiviral envelope vector and pBVIx NF-κB reporter vector were gifted from AKİL Laboratory (Prof. Nesrin Özören).

Table 3.3: Plasmids.

Construct	**Origin**	**Backbone**
T7-RelA-K310R	Addgene #23250	pEv3s
GFP-RelA	Addgene #22122	pEGFP-C1
psPAX2	Addgene #12260	psPAX2
pCMV-VSV-G	Addgene #8454	NA
pBVIx	AKIL Laboratories	NA
pRL-TK-Renilla	Promega # AF025846.2	pRL

Table 3.4: Primers for RT-qPCR.

Primer ID	**Sequence (5'-3')**	**Application**
β-ACTIN-F	TCCTGGGCATGGAGTCCTGT	RT-qPCR
β-ACTIN-R	TCTGCTGGAAGGTGGACAGC	RT-qPCR
K310Rgateway-F	ATGGCTAGCATGACTGGTGGACAGC	Cloning
K310Rgateway-R	TTAGGAGCTGATCTGACTCAGCAG	Cloning

Primers for RT-qPCR were designed on exon-exon junctions of the genes to eliminate genomic DNA amplifications by using GenScript primer design for Real-time PCR tool (USA). Designed primers were ordered from Macrogen (South Korea).

3.3. General Kits, Enzymes and Chemicals

Table 3.5: Kits and Enzymes.

Name	**Supplier**
Caspase 3/7 Assay	Promega, USA
cDNA Synthesis Kit	Bio-Rad, USA
Complete Mini Protease Inhibitor Cocktail	Roche, Switzerland
DC Protein Quantification Assay	Bio-Rad, USA
2-Log DNA Ladder	NEB, UK
ECL-Sirius	Advansta, USA
NucleoBond^{TM} Xtra Midi Plus	Macherey-Nagel, Germany
PageRuler Prestained Protein Ladder	Thermo, USA
PhosStop Phosphatase Inhibitor Coctail	Roche, Switzerland
PVDF Midi RTA Transfer Kit	Bio-Rad, USA
Q5 High-Fidelity DNA Polymerase	NEB, UK
Restriction Endonucleases	Thermo, USA
RNA Extraction Kit	Zymo, USA
SensiFast Sybr	Bioline, UK
T4 DNA Ligase	NEB, UK
XTT Cell Viability Assay	Roche, Germany
Dual-Luciferase Assay	Promega, USA

All the chemicals were ordered from the companies indicated in the table.

Table 3.6: Chemicals.

Chemical	**Supplier**
Acetic Acid	Merck, USA
Acrylamide	AppliChem, Germany
Agarose	Sigma-Aldrich, USA
Ammonium Persulfate (APS)	Sigma-Aldrich, USA
Ampicillin	Roche, Switzerland
Ampicillin	Fluka, USA
APS	AppliChem, Germany
B-Mercaptoethanol	Merck, USA
Boric Acid	Sigma-Aldrich, USA
Bromophenol Blue	Fluka, USA
Calcium chloride dehydrate	AppliChem, Germany
D-Glucose	Sigma-Aldrich, USA
DAPI	AppliChem, Germany
EDTA	AppliChem, Germany
Ethanol	Merck, USA
Ethidium Bromide	Sigma-Aldrich, USA
Glycerol	Sigma-Aldrich, USA
Glycine	Applichem, Germany
HEPES	Sigma-Aldrich, USA
Kanamycin	Emsure, Germany
LB Broth	Caisson Laboratories, USA
LB-Agar	Sigma-Aldrich, USA
Methanol	Merck, USA
Ochratoxin A	Sigma-Aldrich, USA
Paraformaldehyde	Sigma-Aldrich, USA
Phosphate Saline Buffer (PBS)	MPBio, USA
Sodium Chloride (NaCl)	Fisher Scientific, USA

Table 3.6. Chemicals (cont.).

Chemical	Supplier
Sodium Deoxycholate	Sigma-Aldrich, USA
Sodium Dodecyl Sulfate (SDS)	AppliChem, Germany
Sodium Hydroxide	Sigma-Aldrich, USA
TEMED	Sigma-Aldrich, USA
Tris-Base	AppliChem, Germany
Tris-HCl	AppliChem, Germany
Triton X-100	AppliChem, Germany
Tween 20	Sigma-Aldrich, USA
Bay11-7085	Sellekchem, USA

3.4. Western Blot Buffers and Antibodies

After preparation of the buffers, they were stored in aliquots if necessary. RIPA buffer was supplemented with protease inhibitor cocktail and phosphatase inhibitor cocktail before use.

Table 3.7: Western Blot Solutions and Buffers.

Solution/Buffer	Content
RIPA Buffer	150 mM NaCl 1% NP40 0.5% Sodiumdeoxycolate 0.1% SDS 50 mM Tris pH 7.4

Table 3.7. Western Blot Solutions and Buffers (cont.).

Solution/Buffer	**Content**
4XProtein Loading Dye	200mM TrisHCl pH 6.8 8% (w/v) SDS 40% (w/v) 100% Glycerol 4% (w/v) -mercaptoethanol 50 mM EDTA 0.08% (w/v) Bromophenol Blue
12% Resolving Gel	375 mM TrisHCl pH 8.8 0.1% (w/v) SDS Acrylamide:Bisacrylamide (12% w/v) 0.05% (w/v) APS 0.005% (w/v) TEMED
4% Stacking Gel	0.125 mM TrisHCl pH 6.8 0.1% (w/v) SDS Acrylamide:Bisacrylamide (4% w/v) 0.05% (w/v) APS 0.0075% (w/v) TEMED
10X SDS Running Buffer	1% (w/v) SDS 1% (w/v) Tris Base 14.4% (w/v) Glycine
1X Tris Buffered Saline with Tween-20 (TBS-T)	50 mM TrisHCl pH 7.4 150 mM NaCl %0.05 Tween-20
Western Blot Blocking Solution	5% (w/v) skim milk powder TBS-T
1st Antibody Solution	5% (w/v) BSA 0.02% (w/v) Sodium Azide TBS-T

Table 3.7. Western Blot Solutions and Buffers (cont.).

Solution/Buffer	**Content**
2^{nd} Antibody Solution	5% (w/v) skim milk TBS-T'

Table 3.8: Antibodies.

Antibody	**Source**	**Supplier**	**Dilution**
ACTIN (D6A8)	Cell Signalling Technologies, USA	Rabbit	1:1000
AKT (pan) (C67E7)	Cell Signalling Technologies, USA	Rabbit	1:1000
IKBa	Cell Signalling Technologies, USA	Rabbit	1:1000
Mouse IgG, HRP	Cell Signalling Technologies, USA	Rabbit	1:3000
p-AKT (S473) (D9E)	Cell Signalling Technologies, USA	Rabbit	1:1000
p-p44/p42 (T202/Y204)	Cell Signalling Technologies, USA	Rabbit	1:1000
BID	Cell Signalling Technologies, USA	Rabbit	1:1000
p44/42 (Erk1/2) (137F5)	Cell Signalling Technologies, USA	Rabbit	1:1000
SP1	Santa Cruz Biotechnologies, USA	Rabbit	1:1000
p65	Cell Signalling Technologies, USA	Rabbit	1:1000
Rabbit IgG	Cell Signalling Technologies, USA	Rabbit	1:3000

4. METHODS

4.1. Cell Lines and Cell Culture

HK-2 (Human kidney 2) cell line was isolated from adult human kidney, proximal tubules. Cells were immortalized by transducing E6/E7 genes of Human Papilloma Virus (HPV 16) [94]. HK-2 cells obtained from ATCC (American Type Culture Collection), were grown in Dulbecco's Modified Eagle Medium/Nutrient Mixture F-12 (DMEM/F-12) including 10% fetal bovine serum (FBS), 100 U/ml penicillin and 100μg/ml streptomycin. Cells were maintained in an incubator at 37 ^{o}C with 5% CO_2.

4.2. OTA and Inhibitors

OTA was dissolved in ethanol at 10mM final concentration. Stock OTA solution was aliquoted and stored at -80 ^{o}C. Cells were treated with 0.1% v/v ethanol as vehicle control. The treatments were performed in 5% FBS containing DMEM/F-12 medium. Inhibition of certain pathways that are activated upon OTA treatment were achieved by specific inhibitors of key proteins in given pathways. MEK inhibitor, U0126, and IKK inhibitor, Bay11-7085, were used for the inhibition of MEK/ERK1-2 pathway and canonical NF-kB pathway, respectively. U0126 (10 mM) and Bay11-7085 (7.5mM) were dissolved in DMSO and stored at -20 ^{o}C. Cells were seeded in to culture plates (for 96-well plates 8x10^3 cells/100μl medium, for 24-well plates 5x10^4 cells/500μl medium, for 12-well plates 1x10^5 cells/ml, for 6-well plates 2.25x10^5 cells/2ml medium, for 60mm plates 7.5x10^6 cell/3ml medium, for 100mm plates 2.5x10^6 cells /8ml medium, for 150mm plates 6x10^6 cells/17ml medium). Twenty-four hours after seeding, growing medium was replaced with 5% FBS containing assay medium. Cells were treated with OTA (10μM unless stated otherwise) alone or in combination with the inhibitors. Inhibitor treatments (10 μM U0126, 7.5μM Bay11-7085) were performed 1 hour prior to OTA exposure. Cells were treated with 0.1% v/v ethanol or 0.1% v/v ethanol+ 0.1% v/v DMSO as vehicle control of OTA alone or combined treatments respectively.

4.3. Cell Viability Analysis

Cell Proliferation Kit II (XTT analysis) (Roche) was used to determine the effects of OTA and inhibitors on HK-2 cell viability. Basis of the analysis was degradation of yellow-colored tetrazolium salt XTT (sodium 3´-[1-(phenylaminocarbonyl)-3,4-tetrazolium]-bis (4-methoxy-6-nitro) benzene sulfonic acid hydrate) by the dehydrogenase enzyme in the mitochondria of living cells resulting soluble orange-colored formazan that can be detected by microplate reader. Kit was used as recommended by the manufacturer. Briefly, cells ($8x10^3$) were seeded in to 96-well plate and treated with OTA and the inhibitors for 24 hours. After incubation, freshly prepared XTT solution (50μl/well) was added in to the wells and plates were incubated at 37°C, 5% CO_2 environment. After 4 hours of incubation, optical density (OD) values were detected at 490nm and 655nm wavelengths by microplate reader. Average OD values at 655nm of 3 technical replicas were subtracted from average OD values at 490nm of the same technical replicas and experimental results were acquired. Cell viability was calculated as percentage as given in the equation 4.1.

$$CellViability = \frac{SampleValues}{ControlValues} \times 100 \tag{4.1}$$

4.4. Cell Apoptosis Assay

Caspase-Glo®3/7 Assay (Promega) is an assay measuring the activity of caspase-3 and caspase-7 by taking advantage of luminescent substrate. These two enzymes are member of caspase family and have very important roles in driving mammalian cells to apoptosis. Substrate provided in the kit contains DEVD (Asp-GluVal-Asp) tetrapeptide and it has luminogenic property. Addition of Caspase-Glo® 3/7 Reagent causes cell lysis. Active caspases degrade luminogenic substrates and free aminoluciferin. Luciferase enzyme propagate luminescence signal by using the free aminoluciferin as substrate (Figure 4.1) HK-2 cells were seeded on solid bottom white 96-well plate and

treated with OTA and inhibitors for various time points. After the treatments, 100μl Caspase-Glo® 3/7 Reagent was added in to each well and 96-well plate was incubated at room temperature for 30 minutes. After the incubation luminescent signals were detected by luminometer.

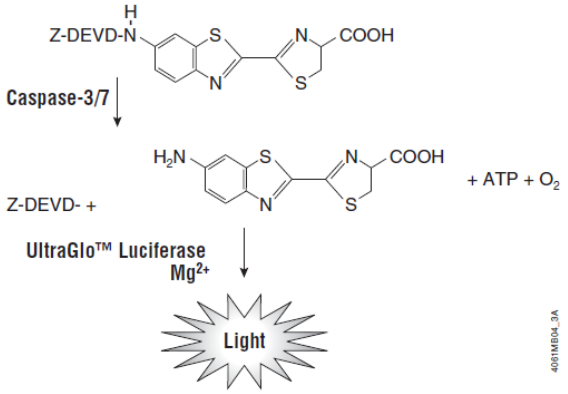

Figure 4.1. Principle of apoptosis analysis

4.5. Transformation and Plasmid Isolation

Competent *Escherichia coli* strains DH5α and Stbl3 were used in transformation. Fifty ng DNA constructs and competent cells were mixed and incubated on ice for 30 minutes. Then bacteria was subjected to heat shock at 42 °C for 90 seconds. Bacteria was incubated on ice again for 5 minutes which was followed by addition of 900μl LB (Luria-Bertani) medium. Bacteria was incubated on thermal-shaker at 37 °C for 1 hour. One-hundred μl of transformed culture was spread on LB-agar plates that has convenient antibiotics. Culture plates were incubated overnight at 37 °C. Following day, formed colonies were picked up with sterile tip and seeded in to 5ml LB media containing proper antibiotics and incubated overnight at 37 °C by shaking. Plasmid isolation was performed by using CTAB method or commercial mini-prep plasmid isolation kit (Machery-Nagel NucleoBond® Xtra Mini kit). Isolated plasmids were cut with proper restriction enzymes for analytic digestion. Uncut and digested plasmids were run on agarose gel for the confirmation of the successful cloning. Bacteria culture was supplemented with 8% glycerol and stored at -80 °C. In order to isolate plasmids

from stock bacteria, starter bacteria from glycerol stock were picked up with the help of a sterile tip and inoculated in to LB medium. The culture was incubated at 37°C for 16 hours by shaking. Plasmids were isolated from culture and concentration of the plasmids was detected by NanoDrop (Thermo Scientific) spectrophotometer. Plasmids were stored at -20 °C.

4.6. Electrophoretic Mobility Shift Assay (EMSA)

4.6.1. Obtaining Nuclear Extracts

Cells were exposed to 10 μM OTA at different time-points (1, 3, 6, 12 and 24 hours) and nuclear extracts were obtained. To achieve that, cells in 100mm plates were washed with 5ml 1x PBS twice and gently scraped from the plates in 1ml PBS. Collected cells were centrifuged at 300g for 2 minutes. Supernatant was discarded. Pellet was resuspended with 400 μl cytosolic lysis buffer (10 mM HEPES pH 7.9, 10 mM KCl, 0.4%v/v NP40, 0.2 mM EDTA, protease inhibitor cocktail (Roche)) and incubated on ice for 15 minutes by shaking. After the incubation cell lysates were centrifuged at 3000g and 4 °C for 3 minutes. Supernatant was saved as cytosolic extract and pellet was resuspended in 200 μl nuclear lysis buffer (20 mM HEPES pH 7.9, 0.4 M NaCl, 10% v/v Glycerol, 1 mM EDTA, protease inhibitor cocktail (Roche)) then sonicated with 40% power 2 cycles for 10 seconds. Lysate was centrifuged at 15,000g and 4 °C for 5 minutes and supernatant was saved as nuclear extract.

4.6.2. 3' End Labelling of the DNA Probes with Biotin

To obtain specific NF-kB–RelA protein binding probe, complementary single strand oligos were ordered from Macrogen (Korea) with sense 5'-AGT TGA GGG GAC TTT CCC AGG CA-3'and anti-sense 5'-GCC TGG GAA AGT CCC CTC AAC TA-3' sequences with one extra adenine nucleotide at 3'-ends. Then, both single strand oligos were mixed together in NEB 2.0 buffer and incubated at 95 °C for 2 minutes. Probes were cooled down slowly to room temperature. Obtained double strand-probes

were labelled with "3' End Labeling Kit" (Thermo Scientific, Catalog No:89818) as recommended by the manufacturer.

4.6.3. Preparing DNA-Protein Complexes

Previously isolated nuclear protein amounts were quantified with commercial DC^{TM} protein assay. Five μg protein was mixed with FastDigest Green Buffer (NEB), 1μM salmon sperm DNA, 100 fmol biotin labelled probes or 2pmol unlabeled probes as control samples in given order. After addition of unlabeled and labelled probes, samples were incubated at RT for 20 minutes. Then protein-probe complexes were loaded on 5% native polyacrylamide gel and run in 0.5X TBE buffer at 100 V for 30 minutes.

4.6.4. Blotting and Crosslinking of Complexes

Complexes in the gel were transferred to positively charged nylon membrane by using Bio-Rad semi-dry blotting device with 3.55mA/cm^2 current for 30 minutes. Membrane containing samples was exposed to 120 mjoule/cm^2 UV light for cross-linking of samples. Membrane was blocked in blocking solution (3% BSA in TBST) for 15 minutes. After blocking, membrane was incubated in Streptavidin-HRP (1:300 v/v) containing blocking solution for 30 minutes and washed with TBST for 5 minutes which was repeated four times. Visualization of the membrane was performed with SynGene G:BOX Chemi XRQ by using WesternBright^{TM} Sirius chemiluminescent detection reagent (Advansta).

4.7. Preparing the Cell Lysates and Western Blot Analysis

Cells were seeded in cell culture plates and treated with OTA and/or inhibitors as described previously in section 4.2. After the treatments, the medium was aspirated, cells were washed with PBS and lysed with RIPA buffer (50 mM Tris-HCl pH 8.0, 150 mM NaCl, 1% NP-40, 0.5% sodium deoxycholate, 0.1% SDS, 1 mM PMSF).

One tablet of PhosSTOP phosphatase inhibitor cocktail (Roche) and 1 tablet cOmplete EDTA-free protease inhibitor cocktail (Roche) were added to every 10ml of RIPA buffer freshly. Cells were lysed in RIPA buffer by incubating on ice for 15 minutes. Lysates were homogenized with the help of 26 gauge syringe and centrifuged at 14000g for 15 minutes at 4 °C. Supernatants were transferred to micro-centrifuge tubes and protein concentrations were measured by using BCA Protein Assay (Thermo Scientific). Equal concetrations of protein lysates were mixed with 4X loading dye (200 mM Tris-HCl pH 6.8, 8% SDS, 40% glycerol, 572 mM β-Mercaptoethanol,mM EDTA, 0.08% bromophenol blue) for loading into SDS-polyacrylamide gels. Protein samples were heated at 95 °C for 5 minutes for denaturation. Ten % polyacrylamide gels with 4% stacking were prepared and placed into tanks filled with 1X SDS Running Buffer(% 1 SDS, 250 mM Tris, 1.92 M glycine). Samples were loaded on the gels and run at 100V until samples reach resolving gels and 120V afterwards for 1-1.5 hours. When electrophoresis was completed, proteins separated according to their sizes were transferred to the PVDF membrane. Transfer was performed by using Bio-Rad Trans-Blot Turbo device with its own commercially available buffer. Blocking was done with 5% w/v skim milk powder in TBS-T (TBS-T: 50 mM TrisHCl pH 7.4, 150 mM NaCl, 0.1% Tween–20) for one hour after the transfer. The membranes were rinsed with TBS-T, 3 times for 5 minutes after blocking. Primary antibody solutions were prepared in 5% BSA w/v in TBS-T solution according to manufacturer's instructions. Membranes were incubated on shaker at 4 °C overnight. Membranes were washed with three times for five minutes after primary antibody incubation and incubated with 1:2500 diluted secondary antibodies (anti-Mouse IgG HRP-linked or anti-Rabbit IgG HRP-linked antibody) (CST) according to the origin of primary antibody for one hour. Membranes were washed with TBS-T three times for five minutes after secondary antibody incubation. Samples were visualized by using WesternBright ECL-HRP substrate or WesternBright Sirius-HRP substrate in SynGene G:BOX Chemi XRQ. Changes in protein levels were analyzed with imageJ (NIH) program.

4.8. Virus Production and Transduction

HEK-293FT cells (7.5 x 10^6) were seeded in to 100mm plate one day before transfection. Cells were transfected with 3 μg of psPAX2 lentiviral packaging vector, 1 μg of pCMV-VSV-G lentiviral envelope vector and 4 μg of lentiviral vector that contains gene of interest by calcium-phosphate transfection method. Two days after the transfection, medium of HEK-293FT cells that contains virus was collected and filtered with 0.45μm filter and divided in to aliquots which was stored at -80 ^{0}C for later usage.

Previously collected 1 ml virus containing medium was mixed with 1 ml fresh medium and 8 μg/ml polybrene to transduce one well of the 6-well culture plate. Eight hours after the addition of the viruses, virus containing medium was replaced with fresh medium. Two days later, infected cells were sorted out either by puromycin treatment or cell sorter depending on the gene they are carrying, puromycin resistance or GFP respectively.

4.9. Detecting NF-κB Transcriptional Activation by Luciferase Assay

HK-2 cells (1x10^5) were seeded on 12-well plates the day before transfection. Cells were co-transfected with two constructs pBVIx, which contains 6x NFκB binding sites in the upstream of firefly luciferase gene, and pRL-TK construct, which has constitutively active TK promoter upstream of Renilla luciferase gene, simultaneously. pGL3 control construct used instead of pBVIx as a positive control. Twenty-four hours after the transfection, cells were treated with OTA for different time periods. Cells were lysed with 100μl 1x passive lysis buffer which was supplied by the kit and plates were incubated at -20 °C for better lysis by freeze-thawing. Cell lysates were thawed on ice and 50μl of sample was transferred to solid-white bottom 96-well plates. FiftyX Stop Glo® reagent was diluted with Stop Glo® buffer to 1x. Fifty μl luciferase assay reagent mix was added on each well and quickly placed in VersaMax plate reader (Molecular Devices, USA) and luminescence signals were detected. Then 50μl Stop Glo® reagent

mix was added on each well and luminescent signals were detected one more time. Second measurements were used for normalization of firefly luciferase measurements. Obtained ratio provided us NF-κB promoter driven gene expression levels.

4.10. Cloning of NFκB Constructs to Lentiviral Backbones

T7-RelA-K310R(23250) and GFP-RelA (23255) plasmids were ordered from Addgene (UK). GFP-RelA insert and pLenti-III-HA lentiviral backbone plasmid were digested with NheI and XbaI (NEB,UK) restriction enzymes. Cut backbone and inserts were ligated with T4-DNA ligase (NEB, UK) and transformed into E. coli Stbl3 competent cells as described in 4.5. Formed colonies were selected and verified with colony PCR by using primers 5'-AAA GGT ACC ATG GCT AGC ATG ACT GG -3' as forward and 5'-TTT TCT AGA TTA GTC GAC GGA TGC CAG-3' as reverse. Positive colonies were grown in liquid LB and plasmids were isolated using Macherey-Nagel NucleoBond® Xtra Midi kit as described in section 4.5.

In order to transfer K310R-RelA insert into lentiviral vector, gateway cloning method was used. K310R primers with gateway recombination sites (5'-GGG GAC AAC TTT GTA CAA AAA AGT TGA TAT GGC TAG CAT GAC TGG TGG ACA GC -3' as forward primer, 5'-GGG GAC AAC TTT GTA CAA GAA AGT TGT TTA GGA GCT GAT CTG ACT CAG CAG -3' as reverse primer) were used to amplify target gene by using T7-K310R RelA (Plasmid 23250) as template. PCR product was run on agarose gel and corresponding band was excised and purified from the gel using MN Gel Extraction Kit. In order to transfer product to the Gateway^{TM} pDONR^{TM}221 Vector, 75ng gel extraction product, 75ng pDONR221 and 1μl BP clonase II enzyme were mixed and ddH_2O added up to 5μl. The mixture was incubated at room temperature overnight. After that, Proteinase K (0.5μl) was added to the mix and the mixture was incubated further at 37 ^{o}C for 15 minutes to stop enzymatic reaction. E.coli Stbl3 competent cells were transformed with gateway ligation mix and grown on kanamycin containing LB plate at 37 ^{o}C for 16 hours. Plasmids were isolated from grown colonies on LB plates. Seventy-five ng of pDONR221 with the gene of interest,

75ng pLVPT and 1μl LR clonase II enzyme were mixed in 5μl total volume and the mix was incubated at room temperature overnight. To stop enzymatic reaction, the mix was treated with Proteinase K (0.5μl) at 37 °C for 15 minutes. E. coli Stbl3 competent cells were transformed with the mix and grown in kanamycin containing LB plate at 37 °C overnight. Plasmids were isolated from grown colonies and digested with BsrGI restriction enzyme to confirm the successful gateway cloning.

4.11. Preparing HK-2 Stable Cell Lines

Cells were transduced as described in section 4.8 with the viruses containing the plasmid constructs prepared in section 4.10. GFP-RelA construct has puromycin resistance gene which allows us to expand the colonies that survive upon puromycin treatment. Non-transduced cells are eliminated with puromycin exposure.

K310R-RelA construct has GFP reporter but doesn't have puromycin resistance gene. Therefore, after transduction, cells were expanded and sorted out with SH800S Cell Sorter (Sony, Japan) according to GFP signal produced by the construct.

4.12. Statistical Analysis

To analyze our experiments Graphpad Prism 6 and Stata 15 softwares were used. Data was shown as avarage ± standart deviations. Comparisons were made with multiple t-test or ANOVA with Bonferroni correction. Significance criteria seek in our test was $p < 0.05$. *$p < 0.05$, **$p < 0.01$, ***$p < 0.001$, ****$p < 0.0001$.

5. RESULTS

Previous members of our group have shown that PI3K/AKT and MAPK/Erk1-2 pathways are activated and remain active for at least 24 hours under OTA exposure [57]. They have also shown that these two pathways work in the opposite directions; PI3K/Akt promotes survival through receptor tyrosine kinase c-Met while MAPK/Erk1-2 is connected to apoptosis [57]. Upstream effector(s) are yet to be clarified. Therefore, previous results indicate that activation of c-Met/PI3K/Akt survival pathway may have roles in carcinogenesis of proximal epithelial cells through suppressing apoptosis initiated by MAPK/Erk1-2 signaling pathway.

Given that OTA is a immunotoxic mycotoxin and knowing that both survival and proapoptotic pathways are activated, the involvement of NF-κB proteins in determining the final outcome of the cells response to OTA is a biologically plausible anticipation.

Based on the data obtained by our group and the literature, our hypothesis is that NF-κB, especially p65 (RelA), is activated when cells exposed to OTA. Subsequently this activation has a role in cells decision-making processes on apoptotic cell death by acting on Erk1-2 phosphorylation.

5.1. Detection of OTA-mediated p65 Translocation to the Nucleus

Until now, nuclear translocation of p65 upon exposure to different OTA concentrations on several cell lines has been shown [92,93]; however, it has not been confirmed in human kidney-2 epithelial (HK-2) human proximal tubular cell line.

As a first step to show NF-κB activation by OTA, nuclear translocation of p65 subunit in HK-2 cells was tested. Therefore, cells were treated with ethanol for 24 hours as vehicle control or 10 μM OTA for 1, 3, 6, 12, and 24 hours. Then cell lysates were fractionated into nuclear and cytoplasmic extracts. The relative levels of proteins

in each fraction were determined by using Western blot analysis. Cross-contamination between the fractions was controlled by examining the presence of BID (cytoplasmic protein) and SP1 (nuclear protein) (Figure 5.1). SP1 and BID bands indicated that the fractionation process was successful. As expected, OTA promotes nuclear translocation of p65 in HK-2 cells starting from 1 hour, peaks at 6 and 12 hours and continues until 24 hour which is the last time point we examined. Densitometric analysis was done by ImageJ and band intensities were quantified (Figure 5.1)

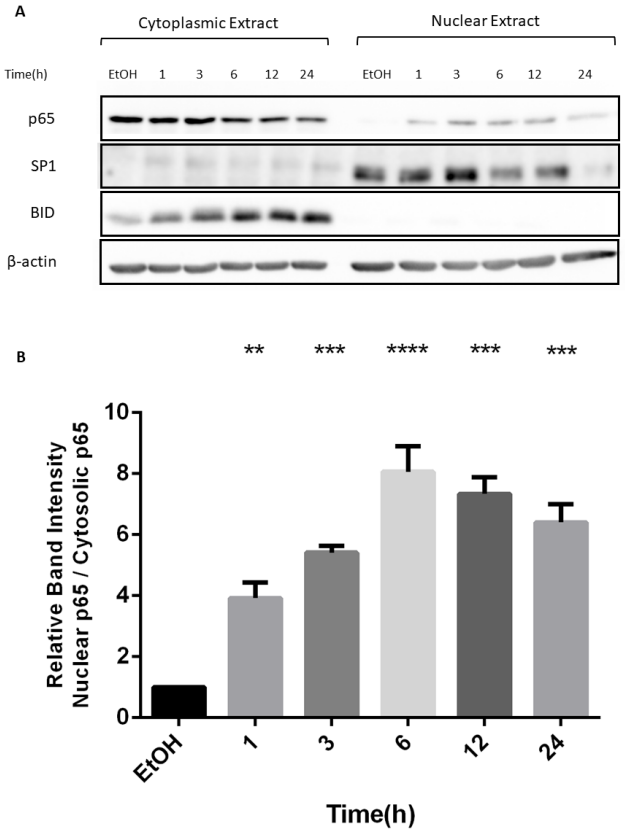

Figure 5.1. Nuclear translocation of p65 upon exposure to OTA was assessed by Western blot. (A) HK-2 cells were treated with 10 μM OTA and EtOH as vehicle for indicated time periods. Cytoplasmic and nuclear fractions were separated and blotted with Western blot (B) Densitometric quantification of Western blots is shown. **p < 0.01, ***p < 0.001, ****p < 0.0001

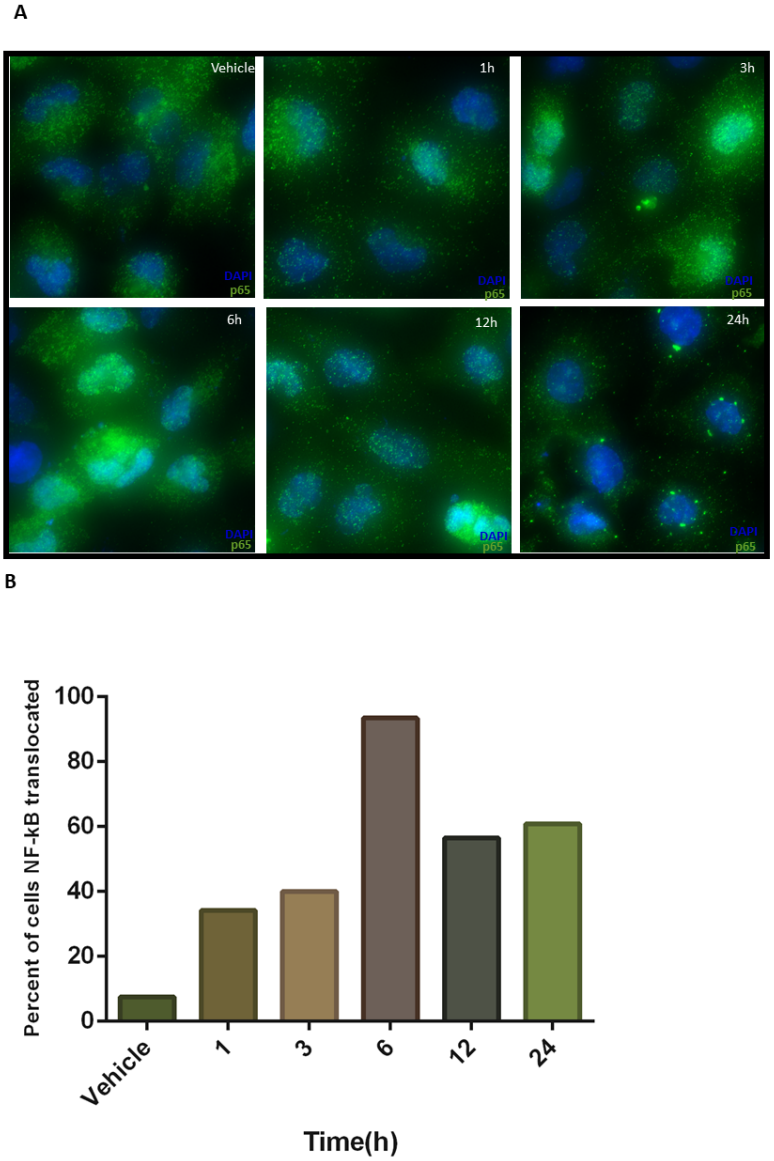

Figure 5.2. Immunoflourescent imaging of p65 translocation upon OTA exposure. (A) GFP-p65 HK-2 cells were treated with 10 μM OTA and EtOH as vehicle. Green signal is emitted from GFP-p65 fusion protein, DAPI stains nucleus and cyan indicates co-localization (B) Percentage of cells that has high nuclear GFP signal.

In order to verify the results, immunoflourescence imaging method was performed where GFP-fused p65 was utilized. Cells stably expressing GFP-p65 fusion protein were seeded on coverslips and treated with 10 μM OTA for 1, 3, 6, 12, 24 hours and EtOH

used as a vehicle control for 24 hours. Cells were fixed with PFA and stained with DAPI. Cells expressing considerable amount of GFP were taken into consideration. High intensity of GFP signal in the nucleus, as evident from the co-localization with DAPI, counted as p65 translocated cells (Figure 5.2). The ratio of the number of cells showing nuclear translocation to the number of cells showing no translocation was calculated and expressed as percentage. Co-localization can be seen as cyan color (Figure 5.2). Here, we observed that the nuclear translocation of p65 starts at as early as 1 hour and peaks at 6 hour when nearly 95% cells displaying translocation and then this percentage regress back to 60% at 12 and 24 hours.

5.2. Detection of DNA Binding Activity of NFκB upon OTA Exposure

In previous section, it was shown that OTA induces p65 nuclear translocation in both HK-2 and GFP-p65 stable HK-2 cells especially peaking at 6 and 12 hours. Thus, we decided to examine whether translocated p65 binds to its target DNA sequence. Biotin labelled DNA probes that contains NFκB-binding sequence were used and electrophoretic mobility shift assay(EMSA) was performed with nuclear lysates from 10 μM OTA treated HK-2 cells. The results show that OTA exposure increases DNA-binding activity of p65. The evidence was provided by showing the shift of protein-DNA complex seen on the EMSA blotting (Figure 5.3). It was observed that amount of shift gradually increase until 12 hour and made a peak, then gradually decreases in accord with the nuclear translocation of p65.

5.3. NF-κB Dependent Gene Expression upon OTA exposure

We have shown that OTA causes translocation of p65 into nucleus. Furthermore the DNA-binding activity of NF-κB was also enhanced especially around 12 hour mark. Therefore, we wondered if this increased DNA-binding is reflected to transcription of NF-κB target genes. pBVIx plasmid containing six NF-κB-binding sites linked to firefly luciferase reporter gene was co-transfected with pRL-TK-renilla luciferase plasmid into HK-2 cells. Results from Dual-Luciferase® Reporter Assay indicate that OTA-

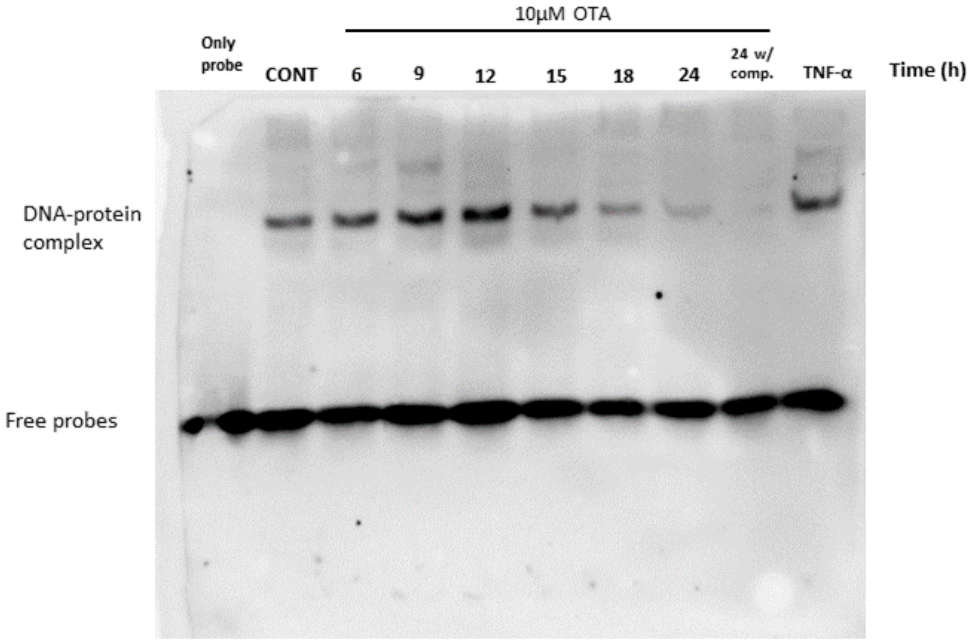

Figure 5.3. DNA-binding of NF-κB upon exposure to OTA evaluated with EMSA analysis. HK-2 cells were treated with 10 μM OTA and EtOH as vehicle, nuclear fractions were used as source of NF-κB in EMSA. Non-labelled probes were used as specific competitors. TNF-α treated cells nuclear extract was used as positive control for NF-κB activation

stimulated NF-κB transcriptional activity increased significantly at 12 hours (Figure 5.4). Twenty four hour treatment also seems to increase NF-κB transcriptional activity even though not significantly. Transfection inefficiency of HK-2 cells may have a negative role in this result.

5.4. Effect of NF-κB on OTA Induced Erk1-2 Phosphorylation

Previous studies from our group have shown that OTA induces Erk1-2 mediated apoptosis [57]. In this study until now, we have shown that OTA also induces NF-κB mediated gene expression. We were curious about whether these two pathways cross-talk. Therefore, we checked phosphorylation state of Erk1-2 in the presence of

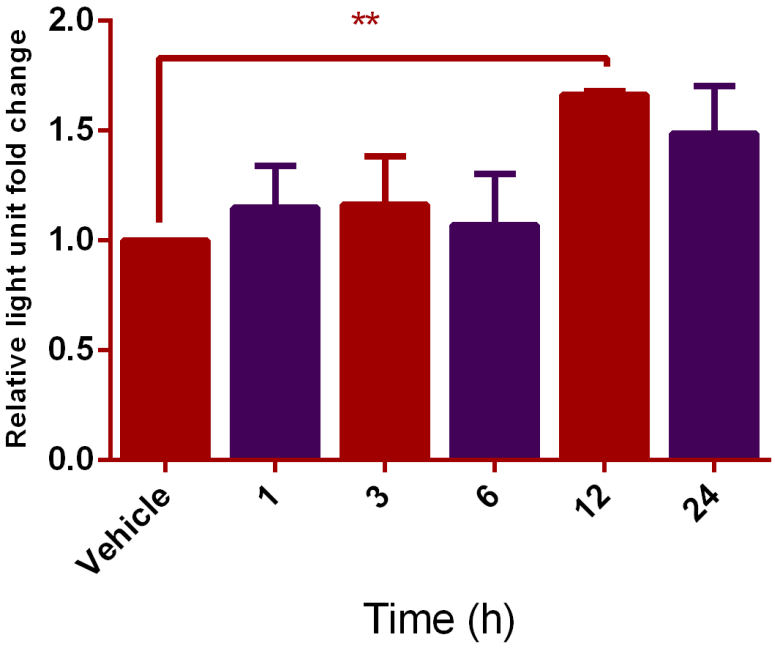

Figure 5.4. Transcriptional activity of NF-κB upon OTA exposure. HK-2 cells were co-transfected with pBVIx and pRL-Renilla constructs as NF-κB activity reporters and treated with 10 μM OTA. EtOH as vehicle control. The results were expressed as relative light unit fold change relative to VHC. **p<0.01

Bay11-7085, an irreversible small molecule inhibitor of IκBα phosphorylation, preventing activation of NF-κB. As seen in the figure 5.5, OTA-mediated Erk1-2 phosphorylation was similar in Bay11-7085 treated and non-treated cells until 6th hour and after that point NF-κB inhibition by Bay11-7085 appeared to reduce OTA-mediated Erk1-2 phosphorylation.

5.5. Cloning of Dominant Negative Form of p65 into Lentiviral Backbone and Generation of Stable HK-2 Cell Lines

After seeing the effects of NF-κB pathway inhibition by Bay11-7085, we decided to generate a stable cell line displaying genetic inhibition. Lysine acetylation at 310th

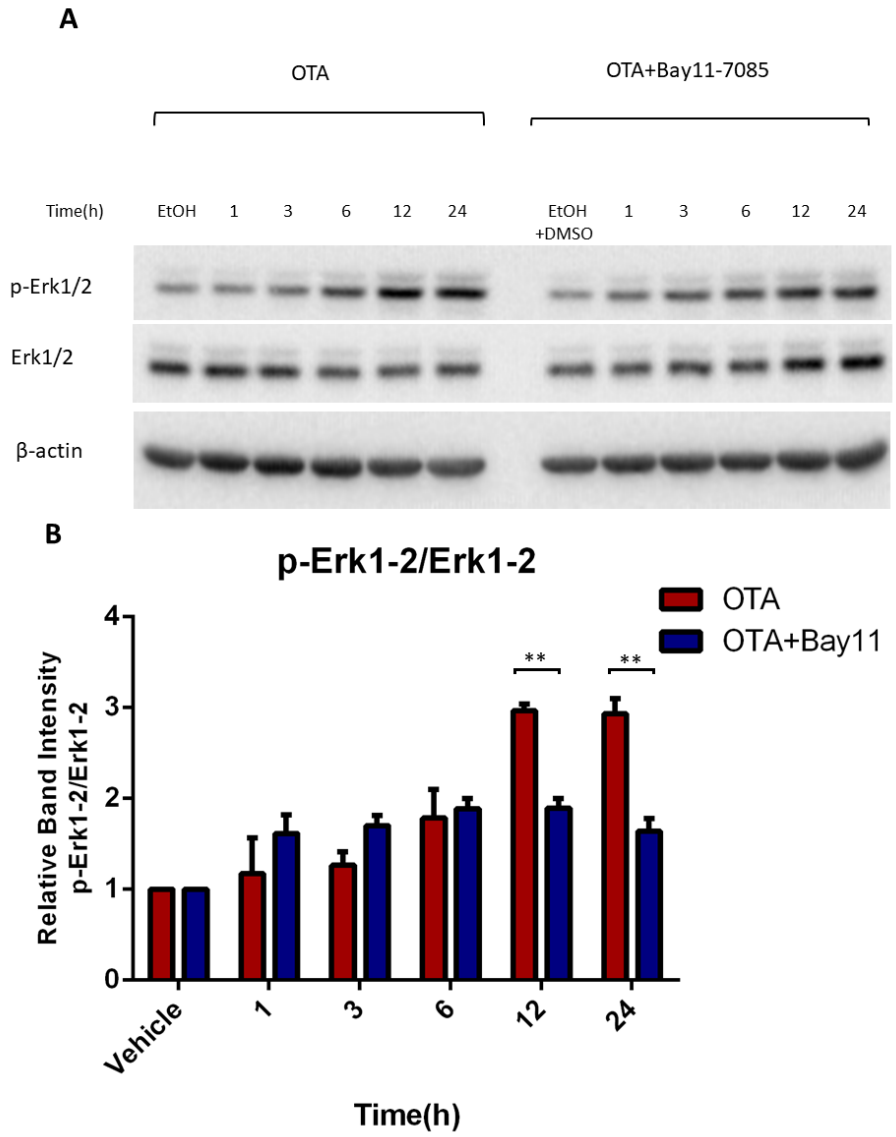

Figure 5.5. Effects of NF-κB pathway inhibition on OTA-mediated Erk1-2 phosphorylation. (A) Cells were treated with 10μM OTA alone or in combination with 7.5μM Bay11-7085, 0.1% EtOH and DMSO were used as vehicle control. Erk phosphorylation evaluated by western blot, β-actin was used as loading control. (B) Densitometric analysis was done by ImageJ. **p<0.01

position was shown to have transcriptional activation role. Acetylation deficient mutant form of p65 at K310 position will bind but would not be able to initiate transcription; thus, we were expecting a dominant-negative effect on NF-κB activity. For this purpose, we ordered T7-RelA(K310R) acetylation deficient p65 and GFP-RelA constructs (Addgene plasmid numbers #23250) and #23255, respectively). In order to generate stable cell line RelA-K310R insert was amplified with PCR (Figure 5.6A) using primers containing adapter sequences for Gateway cloning as described in methods section. PCR products were inserted into pDONR vector with BP reaction. In the figure 5.6B uncut and cut plasmids of six candidate colonies can be seen. After confirming entry of the insert, LR reaction was performed and insert was transferred to the pDEST lentiviral vector (Figure 5.6C).

GFP-RelA and pLENTI plasmids were cut with NheI and XbaI (Figure 5.7A and Figure 5.7B, respectively) and ligated with each other. Since these two enzyme forms compatible sticky ends, colonies that were positive in colony PCR were further confirmed with analytic digestion with KpnI and XbaI restriction enzymes results in nearly 1700 bp fragment when the direction of insert was right(Figure 5.7C). After obtaining GFP-RelA insert in pLENTI-III-HA plasmid, HEK293 cells were transfected to confirm our cloning and expression of p65. It can be seen that when membranes were blotted with anti-p65 antibody non-transfected cells (lane1) have one band near 65 kDa while both GFP-RelA constructs (pEGFPC1 and pLENTI backbones in lanes 2 and 3) have additional band at near 100 kDa that indicates GFP fused p65 protein which is also confirmed with anti-GFP antibody.

5.6. Effect of p65 Inhibition on OTA Induced Apoptosis

Reduction in OTA-induced Erk1-2 phosphorylation by NF-κB inhibition suggests that NF-κB might have a pro-apoptotic role in OTA mode of action. Caspase 3/7 assay and Annexin V staining were used to investigate this hypothesis. Bay11-7085 was given to cells one hour before OTA for every time point and DMSO + EtOH was used as vehicle control for Bay11-7085 samples. Annexin V staining shows that Bay11-7085

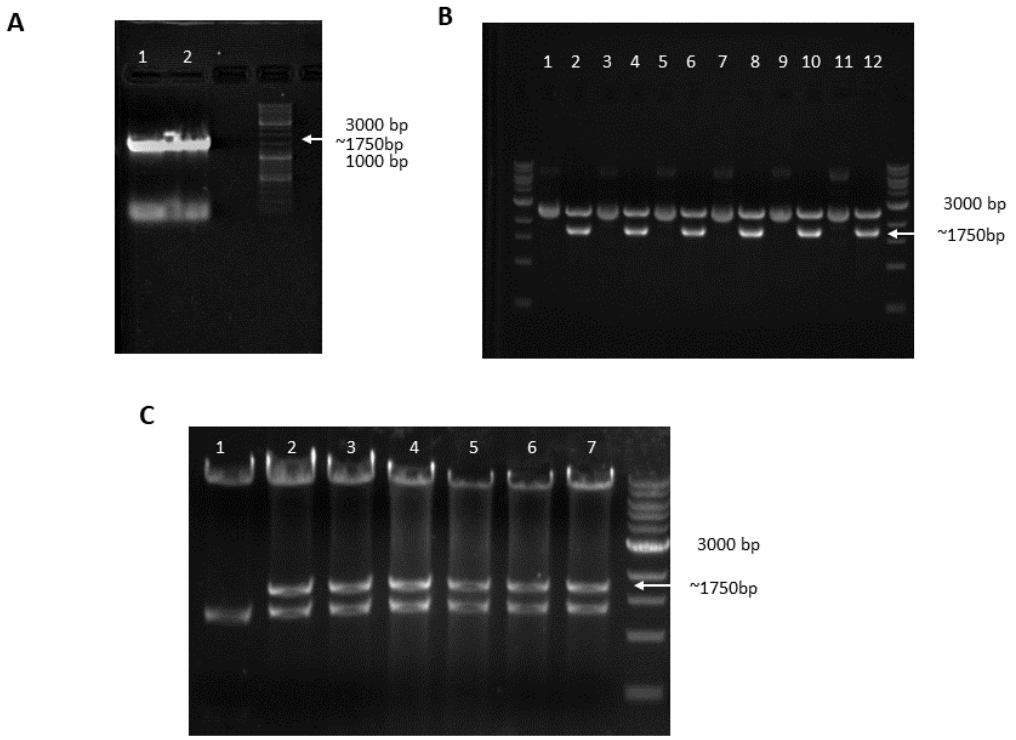

Figure 5.6. Cloning of RelA-K310R into pDEST vector. (A) lanes 1 and 2 PCR amplicons of K310R-RelA. (B) Analytic digestion with BsrGI to test the presence of insert in pDONR; lanes 1, 3, 5, 7, 9, 11 uncut and lanes 2, 4, 6, 8, 10, 12 includes cut plasmids from colonies. (C) Analytic digestion with BsrGI to test the presence of insert in pDEST; lane 1 contains backbone, lanes 2-7 contain plasmids from colonies.

treatment in combination with OTA causes an increase in apoptosis at 3 hour however it decreases apoptosis in 12^{th} hour (Figure 5.8).

5.6.1. Investigating the Role of NF-κB in OTA-Induced Apoptosis by Caspase 3-7 Assay

In order to illustrate the effects of NF-κB pathway inhibition on apoptosis we have performed Caspase3/7 assay with samples that were treated with OTA alone or in combination with Bay11-7085 for indicated time periods. It can be observed that

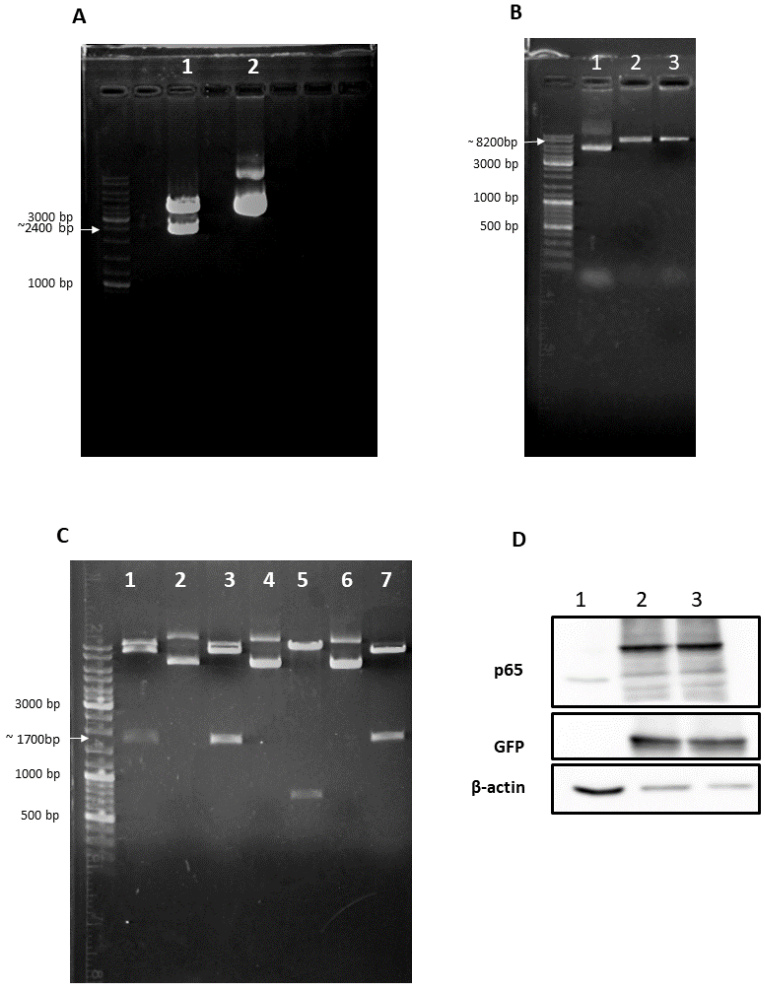

Figure 5.7. Cloning of RelA-GFP to pLENTI-III-HA. (A) GFP-RelA plasmid was digested with NheI/XbaI; lane 1 cut, lane 2 uncut. (B) pLENTI-III-HA plasmids with NheI/XbaI; lane 1 cut, and lane 2 uncut. (C) Validation of cloning; odd lanes were KpnI/XbaI digested, even lanes were uncut plasmids. (D) p65 blot; Lane 1, NT; lane 2, GFP-RelA pEGFPC1; lane3, GFP-RelA in pLENTI transfected cells.

samples treated with only OTA has gradual increase in apoptosis as expected from earlier studies (Figure 5.8). Later time points at 15, 18 and 24th hours Bay11-7085 samples have significant reduction in apoptosis with compared to only OTA samples of corresponding hours (Figure 5.8). This pattern shows similarity to Erk1-2 phosphorylation upon OTA treatments and reducing effect of Bay11-785 on phosphorylation.

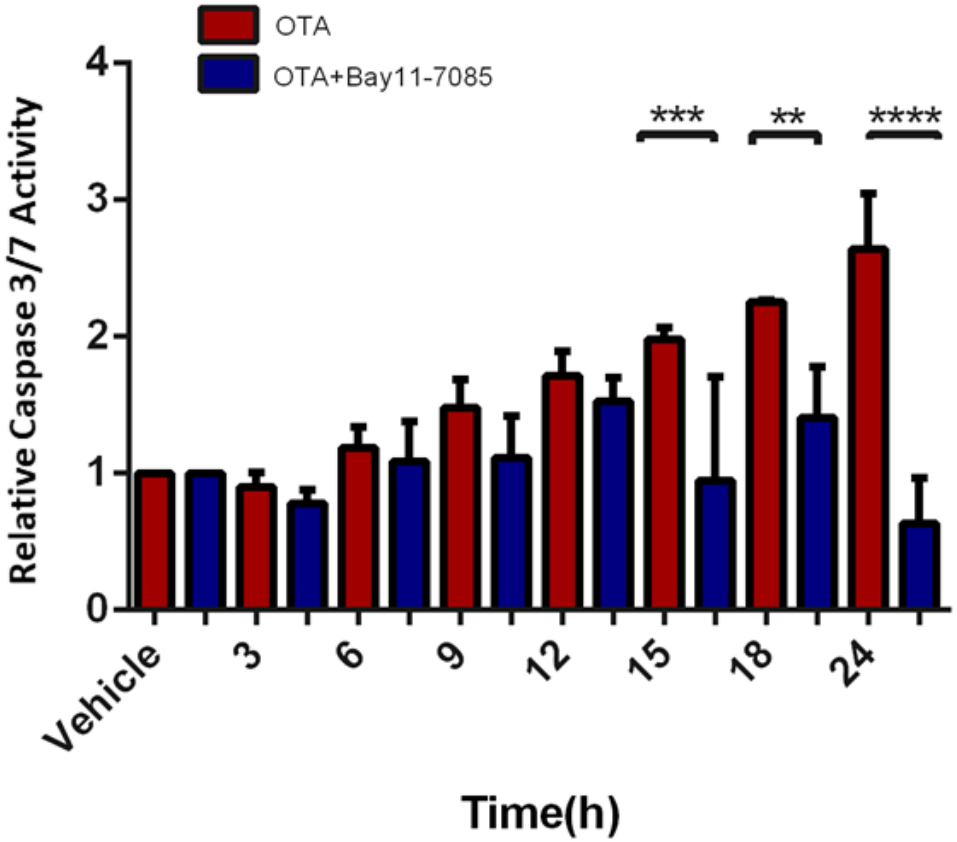

Figure 5.8. Effects of NF-κB pathway inhibitor Bay11-7085 on OTA-induced apoptosis in HK-2 cells. HK-2 Cells were treated with 10 μM OTA alone or in combination with 7.5 μM Bay11-7085 for indicated time periods. Apoptotic activities were detected with Caspase3-7 assay. Results were normalized to vehicle controls. **p<0.01,***p<0.001

Following this result, we tried caspase 3/7 assay with stable cell lines I generated. Instead of Bay11-7085 treatment, RelA-K310R stable cell line was used and GFP-RelA cell line was used as a control group. Two cell lines were treated with 10 μM OTA without NF-κB pathway inhibitor Bay11-7085 at different time points. Unlike inhibition with Bay11-7085, K310R-RelA dominant negative cell line did not show any significant difference compared to GFP-RelA cell line (Figure 5.9). Even though the

expected increase in OTA-mediated apoptosis can be observed in control cells, mutant form of NF-κB could not accomplish significant reduction in apoptotic cell death as seen in Figure 5.9. Twenty four hour results are far below expectation in both control and K310R-RelA cells in terms of apoptotic activity.

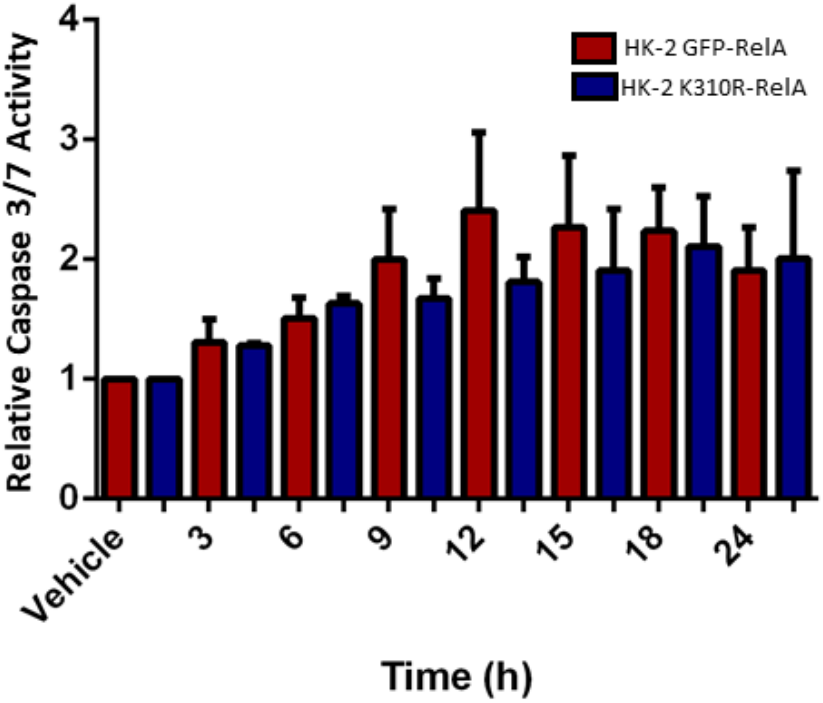

Figure 5.9. Apoptotic effect of OTA on dominant negative p65 expressing K310R-RelA HK-2 cell line. K310R-RelA and GFP-RelA HK-2 cells were treated with 10 μM OTA at designated hours. Apoptotic activities were detected with Caspase3-7 assay. Results were normalized to vehicle controls

5.6.2. Investigation of OTA-induced p65 Dependent Apoptosis by Annexin-V Staining

For further verification, Annexin-V staining technique was used. Annexin V has high affinity towards phosphatidylserine (PS) molecules located in outer leaflet of

apoptotic cell membrane. By utilizing this ability of Annexin V, apoptotic cells can be identified in a cell population with fluorescent dye conjugated Annexin V. Annexin V stained cells then analyzed with flow cytometry to identify apoptotic cells. We have observed a limited increase in apoptotic cells in early time points of OTA treatment whereas a moderate apoptotic response at later time points (12^{th} hour) was inflicted by OTA in HK-2 cells. Inhibition of NF-κB pathway with Bay11-7085 increases apoptotic cell death in the early hours of treatment; however,this increase gradually declines by time. At 12^{th} hour, only OTA treated apoptotic cell ratio was higher than that of OTA+Bay11-7085 treated cells (Figure 5.10)

5.7. Effects of OTA on Erk1-2 phosphorylation in K310R-RelA Stable Cell Line

Since we did not see much difference in caspase 3/7 assay between our stable cell lines, we decided to check individual cells by visualizing p65 under fluorescent microscope by the help of GFP-fused protein and also examining the Erk1-2 phosphorylation by staining cells with phospho-specific Erk1-2 antibody. Moreover, subcellular localization of both proteins and relationship between this two was to be observed.

After treatment with 10 μM OTA treatments for 1, 3, 6, 12 and 24 hours, cells were fixated with PFA and co-stained with anti-p-Erk1-2 and anti-GFP antibodies. Images were taken with DMi8 fluorescent microscope and quantified with ImageJ software (NIH, USA). During quantification two region of interests (ROIs) were determined; first, nucleus boundaries were defined by DAPI signal and second one being cell boundaries, defined by GFP signal. Mean signals from 488 and 568 were measured for both ROIs . Mean of cytoplasmic signal obtained by using equation 5.1

$$CytoplasmicMean = \frac{(TotalMean \times TotalArea) - (NuclearMean \times NuclearArea)}{TotalArea - NuclearArea} \tag{5.1}$$

5.7.1. Effects of OTA on p65 Nuclear Localization in HK-2 K310R-RelA Stable Cells

We quantified the nuclear localization of p65 in individual cells according to their mean signal intensity by utilizing immunocytochemistry. All images were taken with same exposure time, Z-stack number and sizes. The control HK-2 GFP-RelA cells show similar p65 translocation into the nucleus (Figure 5.11A), however, the slight decreases seen in endogenous nuclear/cytoplasmic ratio of p65 at 12^{th} and 24^{th} hours (Figure 5.1) were not observed. Nevertheless, the nature of these two different assays could have caused this small discrepancy. On the other hand, HK-2 K310R-RelA cells have also shown mildly increasing pattern(Figure 5.11B), but this increase was not statistically discernible.

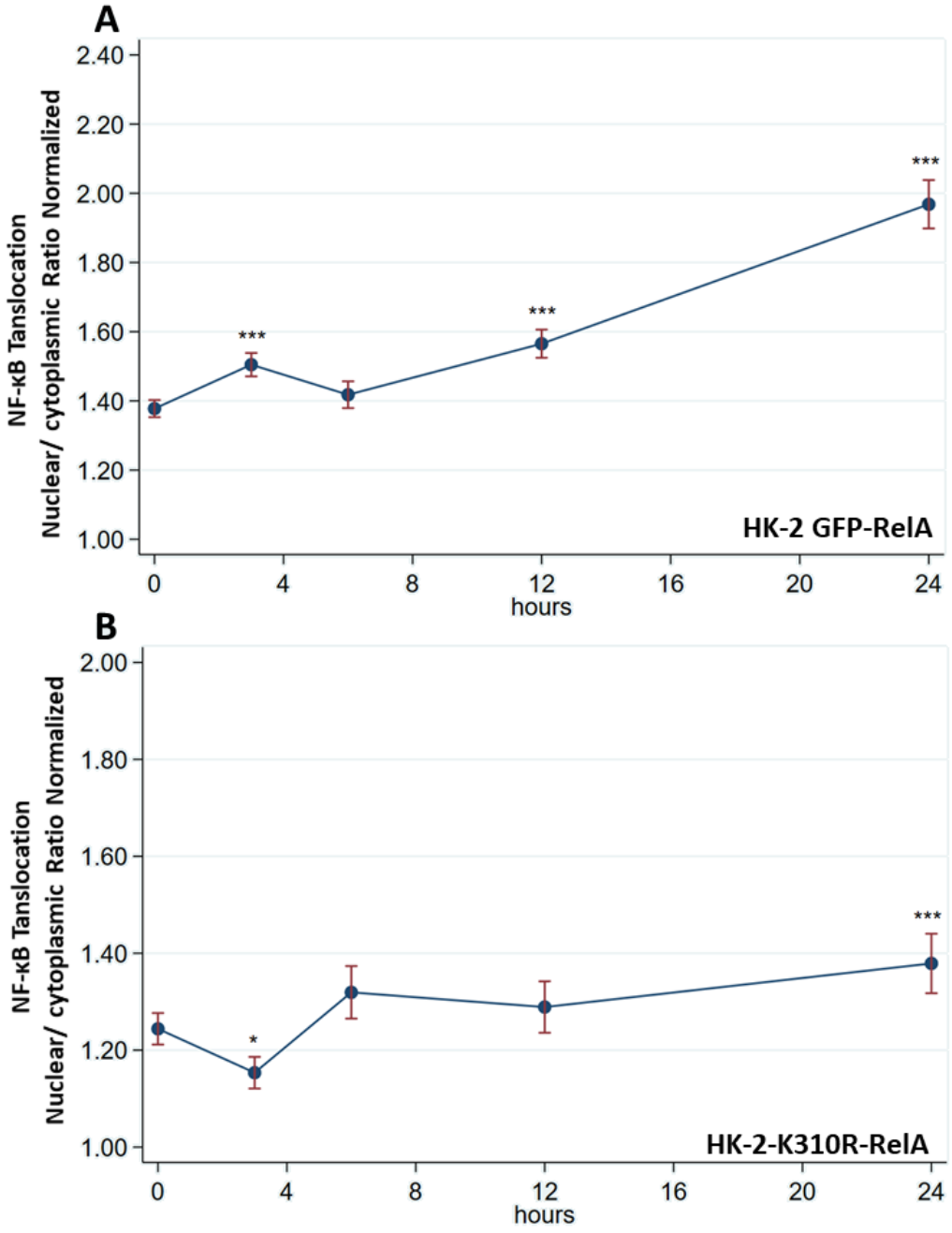

Figure 5.11. Quantification of p65 nuclear localization when K310R-RelA and GFP-RelA HK-2 cells exposed to OTA. Upon 10 μM OTA treatment (A) increased p65 nuclear translocation in HK-2 GFP-RelA cell line and (B) increased p65 nuclear translocation in HK-2 K310R-RelA cell line. *p<0.05,***p<0.001.

5.7.2. Effects of OTA on p-Erk1-2 Nuclear Localization in HK-2 K310R-RelA Stable Cells

Nuclear translocation of p-Erk1-2 was quantified in a manner similar to p65 translocation as described at the beginning of this section. All images were taken with same exposure time, Z-stack number and sizes. Nuclear and cytoplasmic signals of p-Erk1-2 were measured and nuclear/cytoplasmic ratio was calculated as a measure of Erk1-2 translocation. p-Erk1-2 nuclear localization gradually increased in HK-2 GFP-RelA cells and significant difference is observed at 12^{th} and 24^{th} hours with respect to control (Figure 5.12A). On the other hand, nuclear/cytoplasmic ratio of pErk1-2 in K310R-RelA cell line slightly increased at 6^{th} and 12^{th} hours but declined at 24^{th} hour (Figure 5.12) displaying a similar pattern with the p-Erk amount when cells co-treated with Bay11-7085 shown in Figure 5.5.

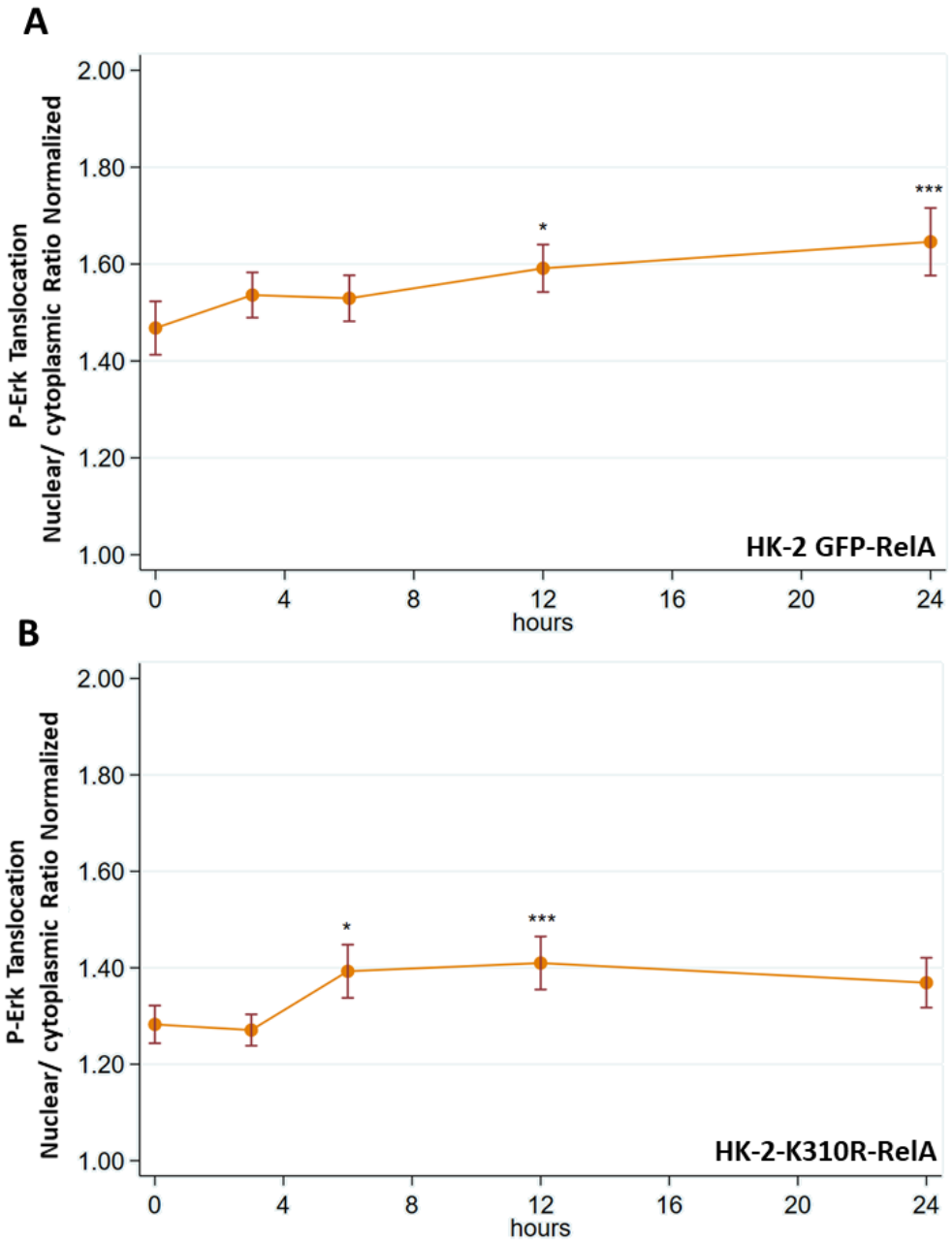

Figure 5.12. Quantification of p-Erk1-2 nuclear localization when K310R-RelA and GFP-RelA HK-2 cells exposed to OTA. Upon 10 μM OTA treatment (A) p-Erk1-2 nuclear translocation in HK-2 GFP-RelA cell line. (B) p-Erk1-2 nuclear translocation in HK-2 K310R-RelA cell line. *p<0.05,***p<0.001.

5.7.3. Investigation of Individual Cells of HK-2 RelA Stable Cell Line Upon OTA Treatment

During stable cell line generation cells were sorted with FACS according to GFP presence. However, every cell has different expression levels because cells were sorted from mix population. I wanted to investigate if there is an effect of varied expression level of dominant-negative form of p65 on Erk1-2 phosphorylation. Overall images resemble signal quantification data obtained in previous sections. Both levels and nuclear to cytoplasmic ratio of p-Erk1-2 increased. Variation in the expression of K310R-RelA mutant seems to have effect on Erk1-2 phosphorylation with compared to GFP-RelA cell line since in the later time-points some individual cells seem to have minuscule amount of signal from red channel 568nm.

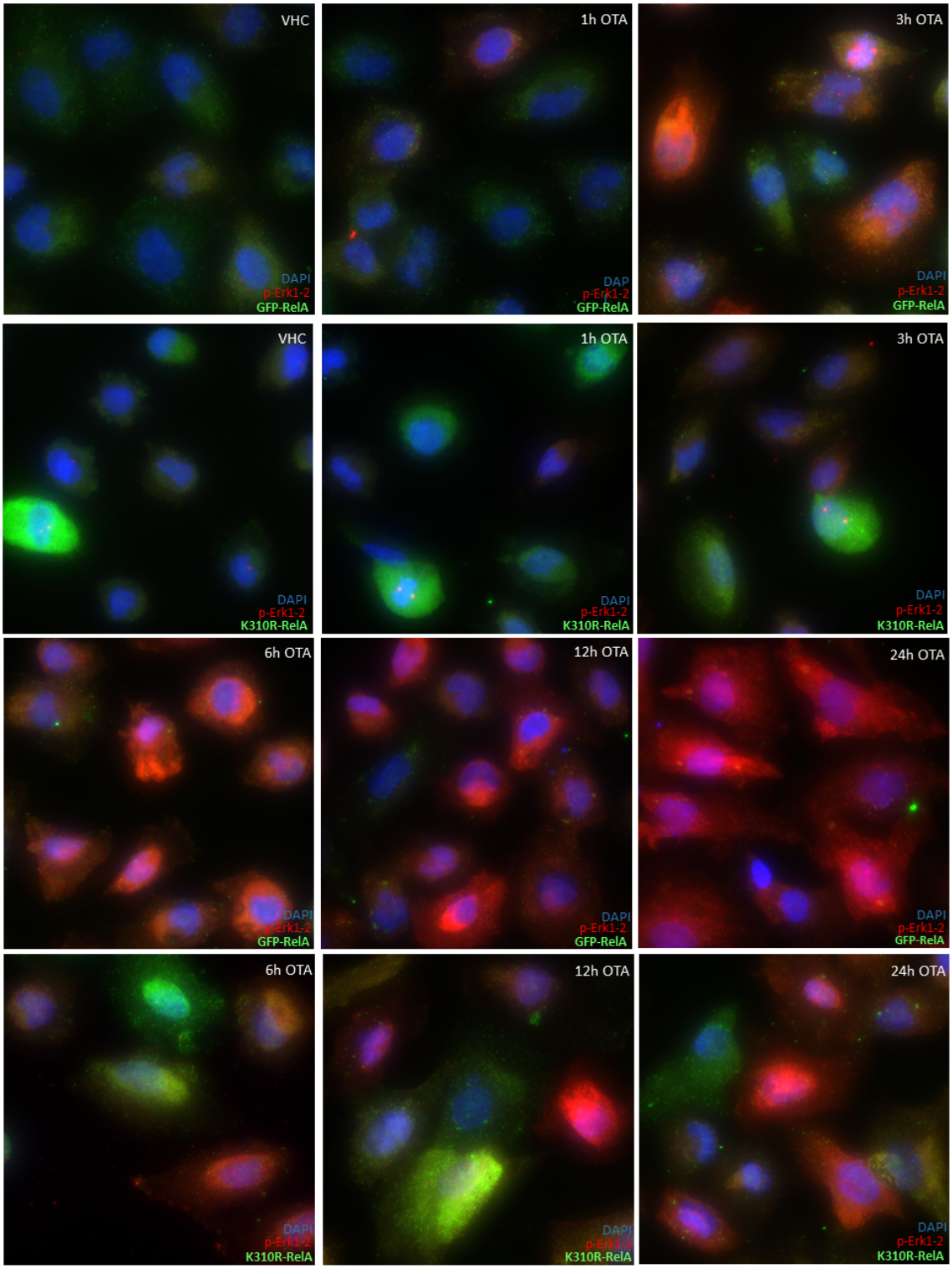

Figure 5.13. Detection p65 and p-Erk localization with immmunofluorescence when K310R-RelA HK-2 cells exposed to OTA. Green signals indicates p65, red signals indicates p-Erk1-2 and blue signal indicates nucleus. GFP-RelA HK-2 cells were used as a control cell line.

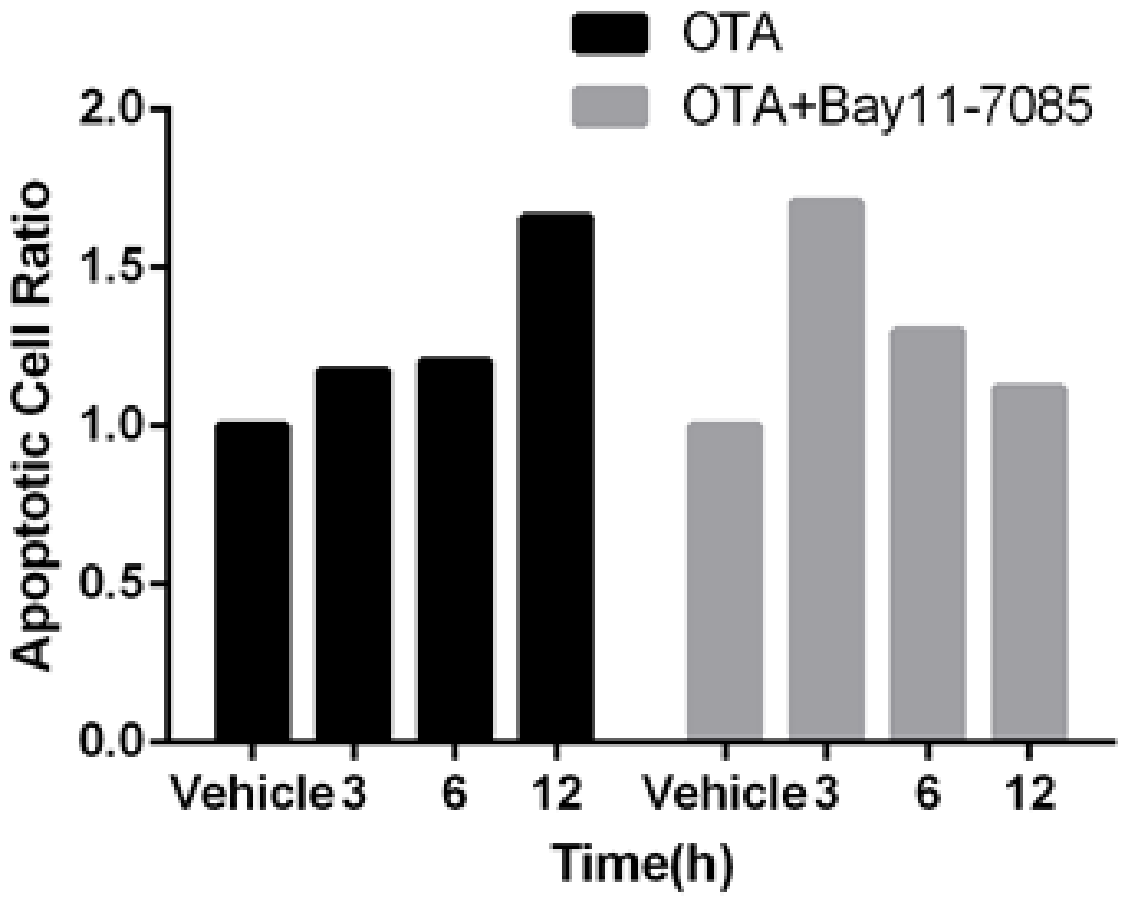

Figure 5.10. Effect of NF-κB pathway inhibitor Bay11-7085 on OTA induced apoptosis in HK-2 cells. Apoptotic cell death detected with Annexin V staining after cells were treated with 10 μM OTA and 7.5 μM Bay11-7085. Results were normalized to vehicle controls.

6. DISCUSSION AND CONCLUSIONS

Ochratoxin A (OTA) is produced by *Aspergillus* and *Penicillium* species of fungi as a secondary metabolite. It contaminates human food and animal feed. As a result of its lengthy half-life and reabsorbtion, it builds up in kidney in prolonged exposures [20]. Carcinogenesis, tumor formation and kidney injury can ensue from chronic exposure to OTA [95]. Balkan Endemic Nephropathy(BEN) is also associated with OTA caused by poor storing conditions of grains [6, 95]. OTA has been shown to have genotoxic and epigenetic effects. Besides, it interferes with numerous signalling pathways [96].

Our group has recently shown that OTA causes sustained activation of MAPK/ Erk1-2 and PI3K/Akt pathways in Human Kidney-2 (HK-2) cell line [57]. These two pathways have opposite impact on cell fate. PI3K/Akt pathway enhances survival response, while MAPK/Erk1-2 pathway increases apoptotic response [97]. OTA mediated PI3K activation was shown to act through receptor tyrosine kinase c-Met [57], however, the upstream effector of Erk1-2 activation has remained to be elucidated.

NF-κB family take roles in various intracellular pathways ranging from immune response to differentiation [58]. Various mycotoxins like altenariol, aflatoxin B_1 [98] among with ochratoxin A [99] were shown to have effects on NF-κB pathways. As mentioned earlier, OTA was shown to increase nuclear translocation of p65 in J774A.1 cell [92] as well as Primary Macaque Kidney (PMK) cells [93]. Rached *et al.* have also shown increased Erk1-2 phosphorylation in parallel with NF-κB activation in IHKE cells [100].

In this Master's thesis, it is demonstrated that OTA increases nuclear shuttling of NF-κB family proteins by Western blottting (Figure 5.1) and florescence imaging (Figure 5.2) in HK-2 cell line, which was previously demonstrated by Ferrante *et al.* in J774A.1 macrophages and Ramyaa *et.al.* in HepG2 liver epithelial cells [101]. Considering that NF-κB is an essential modulator of immune response in cells, it was important

to validate nuclear translocation of NF-κB in our model HK-2 cell line rather than immune cells that can engage NF-κB activation readily. We have used Western blotting (Figure 5.1) and immunocytochemistry (Figure 5.2) to demonstrate the translocation of the p65 subunit of NF-κB. Even though, the magnitudes of nuclear/cytoplasmic p65 ratios are different, both assays show a very similar pattern of p65 translocation.

After illustrating nuclear translocation of NF-κB we have decided to check DNA-binding activity of NF-κB which provides additional validation of nuclear shuttling in consideration using only nuclear extracts in electrophoretic mobility shift assay (EMSA). Moreover, nuclear localization does not directly indicate activation of NF-κB. Acetylation on 221^{th} lysine residue is crucial to κB-enhancer binding of NF-κB [79]. With no surprise, we observed that the DNA-binding activity of NF-κB increases in the presence of OTA (Figure 5.3). Peak points of previous figures and Figure 5.3 were slightly different. This is probably due to the delay between nuclear translocation and DNA-binding activity.

DNA-binding may not directly translate into NF-κB-driven gene expression as well. As mentioned in introduction, acetylation of $310th$ lysine residue affects the transcriptional activation of p65 [79]. Luciferase assays allowed us to validate NF-κB driven gene expression. As other groups have shown [102], transfection efficiency of our model cell line HK-2 was between 30-50% which decreases the sensitivity of the this assay. We observed a statistically significant increase only at 12^{th} hour, however, we strongly believe the 24^{th} hour would also increase significantly. Sauvant *et al.* have shown at least two fold increase in NF-κB activity at 24 hour of 1 μM OTA treatment by using SEAP assay [99]. Even so, these results illustrate that OTA has a significant effect on NF-κB activation and NF-κB-driven gene expression starting from twelve hours.

Our group and others have shown that OTA induces Erk1-2 phosphorylation in different cell lines in time- and dose-dependent manner [57, 100, 103]. Sauvant *et al.* have shown that if Erk1-2 is inhibited that increased NF-κB activity [99] upon OTA

exposure, while Jiang *et al.* claim Erk1-2 inhibition inhibits IL-1β induced NF-κB activation [104]. Another group have claimed that NF-κB inhibits Erk1-2 phosphorylation, however, they only examined the levels of both proteins in cancer cell lines. Faghiri *et al.* have shown that NF-κB inhibition with SN50 downregulates the Erk1-2 phosphorylation when oxidative stress is induced [105] which is a similar case for OTA. Considering these contradictory data, we proceeded to investigate the effect of NF-κB inhibition on OTA-induced Erk1-2 phosphorylation. We observed Erk1-2 phosphorylation when cells were treated with only OTA as shown previously by our group [57]. However, NF-κB pathway inhibitor Bay11-7085 causes a significant reduction in OTA-induced Erk1-2 phosphorylation at 12 and 24 hour in OTA treated cells (Figure 5.5). These results do not directly conflict with indifferences of earlier time-points of luciferase assay results (Figure 5.4), which demonstrates increased NF-κB-driven gene expression after 12 hours of OTA treatment.

Following inhibition of NF-κB pathway with small molecule inhibitor Bay11-7085, we continued on to have genetic inhibition with dominant negative mutation on 310^{th} lysine of p65 to arginine which blocks acetylation on that site allowing mutant p65 proteins to bind to κB enhancer site but inhibiting transcriptional activation of target genes [106]. As mentioned earlier transfection efficiency of HK-2 cells are low, thus we decided to generate stable cell line expressing mutant K310R-RelA . K310R-RelA and GFP-RelA constructs were ordered from Addgene (UK) and cloned into lentiviral vectors as mentioned in section 5.5 (Figure 5.6 and Figure 5.7) for generation of stable cell lines via transduction.

Ozcan *et al.* have shown that OTA increases apoptotic cell death and inhibition of Erk1-2 phosphorylation by MEK inhibitor U0126 mitigates OTA-induced apoptosis in HK-2 cells [57]. On the contrary, recently another group has shown that OTA alone did not cause any increment in apoptotic cell death but OTA induced apoptosis in combination with aflatoxin B in 3D4/21 swine alveolus macrophages demonstrated by Annexin V/PI staining [**?**]. We have tested apoptotic feature of OTA in combination with NF-κB pathway inhibitor Bay11-7085 by employing Annexin V staining (Figure

5.10) and Caspase 3/7 assays (Figure 5.8). Inhibition has a modest effect at 12 hour of OTA exposure but not before that time-point (Figure 5.8) which is consistent with the reduction of OTA-induced Erk1-2 phosphorylation when cells were co-treated with Bay11-7085. Moreover, Xu *et al.* have also shown that OTA provoked apoptosis was restrained with TLR4 inhibition by siRNA transfection, which is one of the upstream effectors of p65 activation [107]. In the caspase3/7 assays, we have demonstrated that NF-κB pathway inhibition with Bay11-7085 causes significant decrease in OTA induced caspase3/7 activity after 15 hours (Figure 5.8). This discrepancy could arise from the fact that Annexin V is an early marker of apoptosis as described in the literature [108] whereas caspase 3 and 7 are effector caspases that are activated in the later stages of apoptosis [109, 110]. Caspase3/7 assays done with K310R-RelA cell line did not demonstrate any significant difference relative to the control cell line (Figure 5.9). This result presumably originate from the insufficient expression of mutant RelA protein all across the population. Figure 5.13 reveals the heterogenous expression in K310R-RelA HK-2 population.

It is known that the NF-κB activation can be analyzed by examining the subcellular localization of p65 from immunofluorescence images. Either the nuclear/cytoplasmic ratio or cytoplasmic - nuclear difference of p65 mean signals can be calculated [111]. We have followed the nucler/cytoplasmic mean signal intensity ratio analysis method, and quantified at least hundred cells in each time point as described with equation 5.1. Significant increase at every time point except 6^{th} hour in control cell line GFP-RelA HK-2 was observed. At 24 hour of treatment (Figure 5.11A), the ratio was around 2.0 which is higher ratio than the TNF-α induction Trask O. used in his experiments as a positive control [111]. Dominant-negative K310R-RelA HK-2 cell line also demonstrated increasing ratio, however, the increase was very modest compared to GFP-RelA HK-2 cells (Figure 5.11B). This result was unexpected, because this mutation is not expected to affect the nuclear translocation of p65. One probable explanation could be the fact that known OTA target genes IL-1β [112] and TNF-α [113] are able to create positive feedback loops with NF-κB [114, 115]. It can be speculated that inhibitory effect of K310R mutation decreased OTA-induced TNF-α and/or IL-1β which in turn

decreased further NF-κB translocation.

p-Erk1-2 translocation is also quantified as nuclear/cytoplasmic ratio. Gradual increase in p-Erk translocation was observed in every time point in GFP-RelA HK-2 cells(Figure 5.12A), Ozcan *et al.* have previously shown OTA-induced Erk1-2 phosphorylation [57] but this is the first time that increased nuclear localization of Erk1-2 is demonstrated under OTA exposure. K310R mutation in p65 shows its effect after 6^{th} hour by limiting the increase in p-Erk translocation and decreasing after 12^{th} hour (Figure 5.12B). This result is in accordance with previous result showing reduction of OTA-mediated Erk1-2 phosphorylation by Bay11-7085 (Figure 5.5).

In the Figure 5.9, K310R-RelA HK-2 cells were failed to show inhibition in OTA-induced apoptosis. we assume underlying reason of this is the low expression levels of dominant-negative form of p65 protein in most cells. Figure 5.13 clearly illustrates individual expression level differences within the cell population. One striking point is that prolonged OTA exposure reduced the phosphorylation of Erk1-2 in cells that have high expression of K310R-RelA while neighbouring cells or conrol cells has distinct and higher p-Erk signal intensity. This confirms our Western blot analysis in Figure 5.5. Moreover, this can also explain why Caspase3/7 assay failed to demonstrate inhibition in apoptosis in K310R-RelA HK-2 cells in Figure 5.9

Altogether these results suggest that NF-κB is activated and translocated to the nucleus upon OTA exposure. Subsequently, the products of NF-κB-dependent gene expression supports Erk1-2 phosphorylation in prolonged OTA exposure and enhance Erk1-2 phosphorylation-dependent apoptosis induction. Inhibition of NF-κB pathway was able to diminish Erk1-2 phosphorylation and apoptosis.

REFERENCES

1. Marin, S., A. Ramos, G. Cano-Sancho and V. Sanchis, "Mycotoxins: Occurrence, toxicology, and exposure assessment", *Food and Chemical Toxicology*, Vol. 60, pp. 218–237, 10 2013.

2. EFSA, *Opinion of the Scientific Panel on contaminants in the food chain related to ochratoxin A*, Tech. Rep. 6, 6 2006.

3. Petzinger, E. and K. Ziegler, "Ochratoxin A from a toxicological perspective.", *Journal of veterinary pharmacology and therapeutics*, Vol. 23, No. 2, pp. 91–8, 4 2000.

4. National Toxicology Program, "Toxicology and Carcinogenesis Studies of Ochratoxin A (CAS No. 303-47-9) in F344/N Rats (Gavage Studies).", *National Toxicology Program technical report series*, Vol. 358, pp. 1–142, 5 1989.

5. Kujawa, M., "Some Naturally Occurring Substances: Food Items and Constituents, Heterocyclic Aromatic Amines and Mycotoxins. IARC Monographs on the Evaluation of Carcinogenic Risks to Humans", *Food / Nahrung*, Vol. 38, No. 3, pp. 351–351, 1 1994.

6. Castegnaro, M., D. Canadas, T. Vrabcheva, T. Petkova-Bocharova, I. N. Chernozemsky and A. Pfohl-Leszkowicz, "Balkan endemic nephropathy: Role of ochratoxins A through biomarkers", *Molecular Nutrition & Food Research*, Vol. 50, No. 6, pp. 519–529, 6 2006.

7. Dai, J., G. Park, J. L. Perry, Y. V. Il'ichev, D. A. J. Bow, J. B. Pritchard, V. Faucet, A. Pfohl-Leszkowicz, R. A. Manderville and J. D. Simon, "Molecular Aspects of the Transport and Toxicity of Ochratoxin A", *Accounts of Chemical Research*, Vol. 37, No. 11, pp. 874–881, 11 2004.

8. Faucet, V., A. Pfohl-Leszkowicz, J. Dai, M. Castegnaro and R. A. Manderville, "Evidence for Covalent DNA Adduction by Ochratoxin A following Chronic Exposure to Rat and Subacute Exposure to Pig", *Chemical Research in Toxicology*, Vol. 17, No. 9, pp. 1289–1296, 9 2004.

9. Jennings-Gee, J. E., M. Tozlovanu, R. Manderville, M. S. Miller, A. Pfohl-Leszkowicz and G. G. Schwartz, "Ochratoxin A: in utero exposure in mice induces adducts in testicular DNA.", *Toxins*, Vol. 2, No. 6, pp. 1428–44, 2010.

10. Arbillaga, L., A. Azqueta, J. H. van Delft and A. López de Cerain, "In vitro gene expression data supporting a DNA non-reactive genotoxic mechanism for ochratoxin A", *Toxicology and Applied Pharmacology*, Vol. 220, No. 2, pp. 216–224, 4 2007.

11. Gautier, J. C., D. Holzhaeuser, J. Markovic, E. Gremaud, B. Schilter and R. J. Turesky, "Oxidative damage and stress response from ochratoxin a exposure in rats.", *Free radical biology & medicine*, Vol. 30, No. 10, pp. 1089–98, 5 2001.

12. Petrik, J., T. Žanić-Grubišić, K. Barišić, S. Pepeljnjak, B. Radić and I. Čepelak, "Apoptosis and oxidative stress induced by ochratoxin A in rat kidney", *Archives of Toxicology*, Vol. 77, No. 12, pp. 685–693, 12 2003.

13. Eder, S., A. Benesic, R. Freudinger, J. Engert, G. Schwerdt, K. Drumm and M. Gekle, "Nephritogenic ochratoxin A interferes with mitochondrial function and pH homeostasis in immortalized human kidney epithelial cells.", *Pflugers Archiv : European journal of physiology*, Vol. 440, No. 4, pp. 521–9, 8 2000.

14. Braunberg, R. C., O. Gantt, C. Barton and L. Friedman, "In vitro effects of the nephrotoxins ochratoxin A and citrinin upon biochemical function of porcine kidney.", *Archives of environmental contamination and toxicology*, Vol. 22, No. 4, pp. 464–70, 5 1992.

15. Marin-Kuan, M., S. Nestler, C. Verguet, C. Bezençon, D. Piguet, T. Delatour and P. Mantle, "MAPK-ERK activation in kidney of male rats chronically fed ochratoxin A at a dose causing a significant incidence of renal carcinoma", *Toxicology and Applied Pharmacology*, Vol. 224, No. 2, pp. 174–181, 10 2007.

16. Van der Merwe, K. J., P. S. Steyn and L. Fourie, "Mycotoxins. II. The constitution of ochratoxins A, B, and C, metabolites of Aspergillus ochraceus Wilh.", *Journal of the Chemical Society. Perkin transactions 1*, pp. 7083–8, 12 1965.

17. World Health Organization, *Evaluation of Certain Food Additives and Contaminants*, Tech. rep., Geneva, 2007.

18. Boudra, H., P. Le Bars and J. Le Bars, "Thermostability of Ochratoxin A in wheat under two moisture conditions.", *Applied and environmental microbiology*, Vol. 61, No. 3, pp. 1156–8, 3 1995.

19. Studer-Rohr, I., *Ochratoxin A in humans: exposure, kinetics and risk assessment*, Ph.D. Thesis, ETH Zürich, 1995.

20. Studer-Rohr, I., J. Schlatter and D. R. Dietrich, "Kinetic parameters and intraindividual fluctuations of ochratoxin A plasma levels in humans.", *Archives of toxicology*, Vol. 74, No. 9, pp. 499–510, 11 2000.

21. Pfohl-Leszkowicz, A. and R. A. Manderville, "Ochratoxin A: An overview on toxicity and carcinogenicity in animals and humans", *Molecular Nutrition & Food Research*, Vol. 51, No. 1, pp. 61–99, 1 2007.

22. Gekle, M., C. Sauvant and G. Schwerdt, "Ochratoxin A at nanomolar concentrations: A signal modulator in renal cells", *Molecular Nutrition & Food Research*, Vol. 49, No. 2, pp. 118–130, 2 2005.

23. Dahlmann, A., W. H. Dantzler, S. Silbernagl and M. Gekle, "Detailed mapping of ochratoxin A reabsorption along the rat nephron in vivo: the nephrotoxin can

be reabsorbed in all nephron segments by different mechanisms.", *The Journal of pharmacology and experimental therapeutics*, Vol. 286, No. 1, pp. 157–62, 7 1998.

24. Schwerdt, G., K. Bauer, M. Gekle and S. Silbernagl, "Accumulation of ochratoxin A in rat kidney in vivo and in cultivated renal epithelial cells in vitro.", *Toxicology*, Vol. 114, No. 3, pp. 177–85, 12 1996.

25. Boorman, G. A., *Toxicology and carcinogenesis studies of ochratoxin A in F344/N rats*, Tech. rep., 5 1989.

26. Boorman, G. A., M. R. Mcdonald, S. Imoto and R. Persing, "Renal Lesions Induced by Ochratoxin A Exposure in the F344 Rat", *Toxicologic Pathology*, Vol. 20, No. 2, pp. 236–245, 2 1992.

27. Bendele, A. M., W. W. Carlton, P. Krogh and E. B. Lillehoj, "Ochratoxin A carcinogenesis in the (C57BL/6J X C3H)F1 mouse.", *Journal of the National Cancer Institute*, Vol. 75, No. 4, pp. 733–42, 10 1985.

28. Baudrimont, I., R. Ahouandjivo and E. E. Creppy, "Prevention of lipid peroxidation induced by ochratoxin A in Vero cells in culture by several agents.", *Chemico-biological interactions*, Vol. 104, No. 1, pp. 29–40, 4 1997.

29. O'Brien, E., A. H. Heussner and D. R. Dietrich, "Species-, sex-, and cell type-specific effects of ochratoxin A and B.", *Toxicological sciences : an official journal of the Society of Toxicology*, Vol. 63, No. 2, pp. 256–64, 10 2001.

30. Sauvant, C., H. Holzinger and M. Gekle, "The Nephrotoxin Ochratoxin A Induces Key Parameters of Chronic Interstitial Nephropathy in Renal Proximal Tubular Cells", *Cellular Physiology and Biochemistry*, Vol. 15, No. 1-4, pp. 125–134, 2005.

31. Kamp, H., G. Eisenbrand, J. Schlatter, K. Wurth and C. Janzowski, "Ochratoxin A: induction of (oxidative) DNA damage, cytotoxicity and apoptosis in mammalian cell lines and primary cells", *Toxicology*, Vol. 206, No. 3, pp. 413–425, 1

2005.

32. Roth, A., G. Eriani, G. Dirheimer and J. Gangloff, "Kinetic properties of pure overproduced Bacillus subtilis phenylalanyl-tRNA synthetase do not favour its in vivo inhibition by ochratoxin A.", *FEBS letters*, Vol. 326, No. 1-3, pp. 87–91, 7 1993.

33. Sinha, K., J. Das, P. B. Pal and P. C. Sil, "Oxidative stress: the mitochondria-dependent and mitochondria-independent pathways of apoptosis", *Archives of Toxicology*, Vol. 87, No. 7, pp. 1157–1180, 7 2013.

34. Trachootham, D., W. Lu, M. A. Ogasawara, N. R.-D. Valle and P. Huang, "Redox Regulation of Cell Survival", *Antioxidants & Redox Signaling*, Vol. 10, No. 8, pp. 1343–1374, 8 2008.

35. Grosse, Y., L. Chekir-Ghedira, A. Huc, S. Obrecht-Pflumio, G. Dirheimer, H. Bacha and A. Pfohl-Leszkowicz, "Retinol, ascorbic acid and alpha-tocopherol prevent DNA adduct formation in mice treated with the mycotoxins ochratoxin A and zearalenone.", *Cancer letters*, Vol. 114, No. 1-2, pp. 225–9, 3 1997.

36. Gautier, J., J. Richoz, D. H. Welti, J. Markovic, E. Gremaud, F. P. Guengerich and R. J. Turesky, "Metabolism of ochratoxin A: absence of formation of genotoxic derivatives by human and rat enzymes.", *Chemical research in toxicology*, Vol. 14, No. 1, pp. 34–45, 1 2001.

37. Tewari, M. and V. M. Dixit, "Fas- and tumor necrosis factor-induced apoptosis is inhibited by the poxvirus crmA gene product.", *The Journal of biological chemistry*, Vol. 270, No. 7, pp. 3255–60, 2 1995.

38. Proskuryakov, S. Y., A. G. Konoplyannikov and V. L. Gabai, "Necrosis: a specific form of programmed cell death?", *Experimental cell research*, Vol. 283, No. 1, pp. 1–16, 2 2003.

39. Lakhani, S. A., A. Masud, K. Kuida, G. A. Porter, C. J. Booth, W. Z. Mehal, I. Inayat and R. A. Flavell, "Caspases 3 and 7: Key Mediators of Mitochondrial Events of Apoptosis", *Science*, Vol. 311, No. 5762, pp. 847–851, 2 2006.

40. Ba, X. and N. J. Garg, "Signaling Mechanism of Poly(ADP-Ribose) Polymerase-1 (PARP-1) in Inflammatory Diseases", *The American Journal of Pathology*, Vol. 178, No. 3, pp. 946–955, 3 2011.

41. Luhe, A., H. Hildebrand, U. Bach, T. Dingermann and H.-J. Ahr, "A New Approach to Studying Ochratoxin A (OTA)-Induced Nephrotoxicity: Expression Profiling in Vivo and in Vitro Employing cDNA Microarrays", *Toxicological Sciences*, Vol. 73, No. 2, pp. 315–328, 6 2003.

42. Müller, G., P. Kielstein, H. Köhler, A. Berndt and H. Rosner, "Studies of the influence of ochratoxin A on immune and defense reactions in the mouse model.", *Mycoses*, Vol. 38, No. 1-2, pp. 85–91.

43. Hassan, Z. U., M. Z. Khan, M. K. Saleemi, A. Khan, I. Javed and M. Noreen, "Immunological responses of male White Leghorn chicks kept on ochratoxin A (OTA)-contaminated feed", *Journal of Immunotoxicology*, Vol. 9, No. 1, pp. 56–63, 3 2012.

44. Haubeck, H. D., G. Lorkowski, E. Kölsch and R. Röschenthaler, "Immunosuppression by ochratoxin A and its prevention by phenylalanine.", *Applied and environmental microbiology*, Vol. 41, No. 4, pp. 1040–2, 4 1981.

45. Lea, T., K. Steien and F. C. Stormer, *Mechanism of ochratoxin A-induced immunosuppression*, Tech. Rep. 9, 1989.

46. Luster, M. I., D. R. Germolec, G. R. Burleson, C. W. Jameson, M. F. Ackermann, K. R. Lamm and H. T. Hayes, *Selective Immunosuppression in Mice of Natural Killer Cell Activity by Ochratoxin A*, Tech. rep., 1987.

47. Cremer, B., A. Soja, J.-A. Sauer and M. Damm, "Pro-inflammatory effects of ochratoxin A on nasal epithelial cells", *European Archives of Oto-Rhino-Laryngology*, Vol. 269, No. 4, pp. 1155–1161, 4 2012.

48. Weston, C. R. and R. J. Davis, "The JNK signal transduction pathway.", *Current opinion in genetics & development*, Vol. 12, No. 1, pp. 14–21, 2 2002.

49. Dhillon, A. S., S. Hagan, O. Rath and W. Kolch, "MAP kinase signalling pathways in cancer", *Oncogene*, Vol. 26, No. 22, pp. 3279–3290, 5 2007.

50. Cargnello, M. and P. P. Roux, "Activation and function of the MAPKs and their substrates, the MAPK-activated protein kinases.", *Microbiology and molecular biology reviews : MMBR*, Vol. 75, No. 1, pp. 50–83, 3 2011.

51. Hanahan, D. and R. A. Weinberg, "The hallmarks of cancer.", *Cell*, Vol. 100, No. 1, pp. 57–70, 1 2000.

52. Yamamoto, T., M. Ebisuya, F. Ashida, K. Okamoto, S. Yonehara and E. Nishida, "Continuous ERK Activation Downregulates Antiproliferative Genes throughout G1 Phase to Allow Cell-Cycle Progression", *Current Biology*, Vol. 16, No. 12, pp. 1171–1182, 6 2006.

53. Mirza, A. M., S. Gysin, N. Malek, K.-i. Nakayama, J. M. Roberts and M. McMahon, "Cooperative Regulation of the Cell Division Cycle by the Protein Kinases RAF and AKT", *Molecular and Cellular Biology*, Vol. 24, No. 24, pp. 10868–10881, 12 2004.

54. Jo, S.-K., W. Y. Cho, S. A. Sung, H. K. Kim and N. H. Won, "MEK inhibitor, U0126, attenuates cisplatin-induced renal injury by decreasing inflammation and apoptosis", *Kidney International*, Vol. 67, No. 2, pp. 458–466, 2 2005.

55. Wang, X., J. L. Martindale and N. J. Holbrook, "Requirement for ERK Activation in Cisplatin-induced Apoptosis", *Journal of Biological Chemistry*, Vol. 275,

No. 50, pp. 39435–39443, 12 2000.

56. Subramaniam, S., U. Zirrgiebel, O. von Bohlen und Halbach, J. Strelau, C. Laliberté, D. R. Kaplan and K. Unsicker, "ERK activation promotes neuronal degeneration predominantly through plasma membrane damage and independently of caspase-3", *The Journal of Cell Biology*, Vol. 165, No. 3, pp. 357–369, 5 2004.

57. Özcan, Z., G. Gül and I. Yaman, "Ochratoxin A activates opposing c-MET/PI3K/Akt and MAPK/ERK 1-2 pathways in human proximal tubule HK-2 cells", *Archives of Toxicology*, Vol. 89, No. 8, pp. 1313–1327, 8 2015.

58. Oeckinghaus, A. and S. Ghosh, "The NF-kappaB family of transcription factors and its regulation.", *Cold Spring Harbor perspectives in biology*, Vol. 1, No. 4, p. a000034, 10 2009.

59. Hoffmann, A., T. H. Leung and D. Baltimore, "Genetic analysis of NF- B/Rel transcription factors defines functional specificities", *The EMBO Journal*, Vol. 22, No. 20, pp. 5530–5539, 10 2003.

60. Hayden, M. S. and S. Ghosh, "Shared Principles in NF-κB Signaling", *Cell*, Vol. 132, No. 3, pp. 344–362, 2 2008.

61. Perkins, N. D., "Post-translational modifications regulating the activity and function of the nuclear factor kappa B pathway", *Oncogene*, Vol. 25, No. 51, pp. 6717–6730, 10 2006.

62. Ghosh, S. and M. Karin, "Missing Pieces in the NF-κB Puzzle", *Cell*, Vol. 109, No. 2, pp. S81–S96, 4 2002.

63. Chen, L.-F. and W. C. Greene, "Shaping the nuclear action of NF-κB", *Nature Reviews Molecular Cell Biology*, Vol. 5, No. 5, pp. 392–401, 5 2004.

64. Huang, B., X.-D. Yang, A. Lamb and L.-F. Chen, "Posttranslational modifications

of NF-κB: another layer of regulation for NF-κB signaling pathway", *Cellular signalling*, Vol. 22, No. 9, p. 1282, 2010.

65. Zhong, H., R. E. Voll and S. Ghosh, "Phosphorylation of NF-κB p65 by PKA Stimulates Transcriptional Activity by Promoting a Novel Bivalent Interaction with the Coactivator CBP/p300", *Molecular Cell*, Vol. 1, No. 5, pp. 661–671, 4 1998.

66. Jamaluddin, M., S. Wang, I. Boldogh, B. Tian and A. R. Brasier, "TNF-α-induced NF-κB/RelA Ser276 phosphorylation and enhanceosome formation is mediated by an ROS-dependent PKAc pathway", *Cellular Signalling*, Vol. 19, No. 7, pp. 1419–1433, 7 2007.

67. Sakurai, H., H. Chiba, H. Miyoshi, T. Sugita and W. Toriumi, "IkappaB kinases phosphorylate NF-kappaB p65 subunit on serine 536 in the transactivation domain.", *The Journal of biological chemistry*, Vol. 274, No. 43, pp. 30353–6, 10 1999.

68. Buss, H., A. Dörrie, M. L. Schmitz, R. Frank, M. Livingstone, K. Resch and M. Kracht, "Phosphorylation of Serine 468 by GSK-3β Negatively Regulates Basal p65 NF-κB Activity", *Journal of Biological Chemistry*, Vol. 279, No. 48, pp. 49571–49574, 11 2004.

69. Mattioli, I., H. Geng, A. Sebald, M. Hodel, C. Bucher, M. Kracht and M. L. Schmitz, "Inducible Phosphorylation of NF-κB p65 at Serine 468 by T Cell Costimulation Is Mediated by IKK", *Journal of Biological Chemistry*, Vol. 281, No. 10, pp. 6175–6183, 3 2006.

70. Bohuslav, J., L.-f. Chen, H. Kwon, Y. Mu and W. C. Greene, "p53 Induces NF-κB Activation by an IκB Kinase-independent Mechanism Involving Phosphorylation of p65 by Ribosomal S6 Kinase 1", *Journal of Biological Chemistry*, Vol. 279, No. 25, pp. 26115–26125, 6 2004.

71. Chen, L.-F., S. A. Williams, Y. Mu, H. Nakano, J. M. Duerr, L. Buckbinder and W. C. Greene, "NF- B RelA Phosphorylation Regulates RelA Acetylation", *Molecular and Cellular Biology*, Vol. 25, No. 18, pp. 7966–7975, 9 2005.

72. Hoberg, J. E., A. E. Popko, C. S. Ramsey and M. W. Mayo, "I B Kinase - Mediated Derepression of SMRT Potentiates Acetylation of RelA/p65 by p300", *Molecular and Cellular Biology*, Vol. 26, No. 2, pp. 457–471, 1 2006.

73. Geng, H., T. Wittwer, O. Dittrich-Breiholz, M. Kracht and M. L. Schmitz, "Phosphorylation of NF-κB p65 at Ser468 controls its COMMD1-dependent ubiquitination and target gene-specific proteasomal elimination", *EMBO reports*, Vol. 10, No. 4, pp. 381–386, 4 2009.

74. Anrather, J., G. Racchumi and C. Iadecola, "cis -Acting Element-specific Transcriptional Activity of Differentially Phosphorylated Nuclear Factor-κB", *Journal of Biological Chemistry*, Vol. 280, No. 1, pp. 244–252, 1 2005.

75. Duran, A., "Essential role of RelA Ser311 phosphorylation by PKC in NF- B transcriptional activation", *The EMBO Journal*, Vol. 22, No. 15, pp. 3910–3918, 8 2003.

76. O'Shea, J. and N. Perkins, "Thr435 phosphorylation regulates RelA (p65) NF-κB subunit transactivation", *Biochemical Journal*, Vol. 426, No. 3, pp. 345–354, 3 2010.

77. Rocha, S., M. D. Garrett, K. J. Campbell, K. Schumm and N. D. Perkins, "Regulation of NF-κB and p53 through activation of ATR and Chk1 by the ARF tumour suppressor", *The EMBO Journal*, Vol. 24, No. 6, pp. 1157–1169, 3 2005.

78. Kiernan, R., V. Brès, R. W. M. Ng, M.-P. Coudart, S. El Messaoudi, C. Sardet, D.-Y. Jin, S. Emiliani and M. Benkirane, "Post-activation Turn-off of NF-κB-dependent Transcription Is Regulated by Acetylation of p65", *Journal of Biolog-*

ical Chemistry, Vol. 278, No. 4, pp. 2758–2766, 1 2003.

79. Chen, L.-f., Y. Mu and W. C. Greene, "Acetylation of RelA at discrete sites regulates distinct nuclear functions of NF-kappaB.", *The EMBO journal*, Vol. 21, No. 23, pp. 6539–48, 12 2002.

80. Kiernan, R., V. Brès, R. W. M. Ng, M.-P. Coudart, S. El Messaoudi, C. Sardet, D.-Y. Jin, S. Emiliani and M. Benkirane, "Post-activation Turn-off of NF-κB-dependent Transcription Is Regulated by Acetylation of p65", *Journal of Biological Chemistry*, Vol. 278, No. 4, pp. 2758–2766, 1 2003.

81. Buerki, C., K. M. Rothgiesser, T. Valovka, H. R. Owen, H. Rehrauer, M. Fey, W. S. Lane and M. O. Hottiger, "Functional relevance of novel p300-mediated lysine 314 and 315 acetylation of RelA/p65.", *Nucleic acids research*, Vol. 36, No. 5, pp. 1665–80, 3 2008.

82. Yang, X.-D., B. Huang, M. Li, A. Lamb, N. L. Kelleher and L.-F. Chen, "Negative regulation of NF-κB action by Set9-mediated lysine methylation of the RelA subunit", *The EMBO Journal*, Vol. 28, No. 8, pp. 1055–1066, 4 2009.

83. Ea, C.-K. and D. Baltimore, "Regulation of NF-κB activity through lysine monomethylation of p65", *Proceedings of the National Academy of Sciences*, Vol. 106, No. 45, pp. 18972–18977, 11 2009.

84. Khosravi-Far, R. and E. White, *reProgrammed Cell Death in Cancer Progression and Therapyf*, Springer, Boston, 1 edn., 2008.

85. Zheng, L., N. Bidere, D. Staudt, A. Cubre, J. Orenstein, F. K. Chan and M. Lenardo, "Competitive control of independent programs of tumor necrosis factor receptor-induced cell death by TRADD and RIP1.", *Molecular and cellular biology*, Vol. 26, No. 9, pp. 3505–13, 5 2006.

86. Edinger, A. L. and C. B. Thompson, "Death by design: apoptosis, necrosis and

autophagy", *Current Opinion in Cell Biology*, Vol. 16, No. 6, pp. 663–669, 12 2004.

87. Campbell, K. J., S. Rocha and N. D. Perkins, "Active Repression of Antiapoptotic Gene Expression by RelA(p65) NF-κB", *Molecular Cell*, Vol. 13, No. 6, pp. 853–865, 3 2004.

88. Kimura, M., M. Haisa, H. Uetsuka, M. Takaoka, T. Ohkawa, R. Kawashima, T. Yamatsuji, M. Gunduz, Y. Kaneda, N. Tanaka and Y. Naomoto, "TNF combined with IFN-α accelerates NF-κB-mediated apoptosis through enhancement of Fas expression in colon cancer cells", *Cell Death & Differentiation*, Vol. 10, No. 6, pp. 718–728, 6 2003.

89. Wiener, Z., E. C. Ontsouka, S. Jakob, R. Torgler, A. Falus, C. Mueller and T. Brunner, "Synergistic induction of the Fas (CD95) ligand promoter by Max and NFκB in human non-small lung cancer cells", *Experimental Cell Research*, Vol. 299, No. 1, pp. 227–235, 9 2004.

90. Ravi, R., G. C. Bedi, L. W. Engstrom, Q. Zeng, B. Mookerjee, C. Gélinas, E. J. Fuchs and A. Bedi, "Regulation of death receptor expression and TRAIL/Apo2L-induced apoptosis by NF-κB", *Nature Cell Biology*, Vol. 3, No. 4, pp. 409–416, 4 2001.

91. Hou, L., F. Gan, X. Zhou, Y. Zhou, G. Qian, Z. Liu and K. Huang, "Immunotoxicity of ochratoxin A and aflatoxin B1 in combination is associated with the nuclear factor kappa B signaling pathway in 3D421 cells", *Chemosphere*, Vol. 199, pp. 718–727, 5 2018.

92. Ferrante, M., G. M. Raso, M. Bilancione, E. Esposito, A. Iacono and R. Meli, "Differential modification of inflammatory enzymes in J774A.1 macrophages by ochratoxin A alone or in combination with lipopolysaccharide", *Toxicology Letters*, Vol. 181, No. 1, pp. 40–46, 9 2008.

93. Kumar, R., S. Alam, B. P. Chaudhari, P. D. Dwivedi, S. K. Jain, K. M. Ansari and M. Das, "Ochratoxin A-induced cell proliferation and tumor promotion in mouse skin by activating the expression of cyclin-D1 and cyclooxygenase-2 through nuclear factor-kappa B and activator protein-1", *Carcinogenesis*, Vol. 34, No. 3, pp. 647–657, 3 2013.

94. Ryan, M. J., G. Johnson, J. Kirk, S. M. Fuerstenberg, R. A. Zager and B. Torok-Storb, "HK-2: an immortalized proximal tubule epithelial cell line from normal adult human kidney.", *Kidney international*, Vol. 45, No. 1, pp. 48–57, 1 1994.

95. Maaroufi, K., A. Pfohl-Leszkowicz, A. Achour, M. el May, Y. Grosse, M. Hammami, F. Ellouz, E. E. Creppy and H. Bacha, "Ochratoxin A genotoxicity, relation to renal tumors.", *Archives de l'Institut Pasteur de Tunis*, Vol. 71, No. 1-2, pp. 21–31.

96. Heussner, A. and L. Bingle, "Comparative Ochratoxin Toxicity: A Review of the Available Data", *Toxins*, Vol. 7, No. 10, pp. 4253–4282, 10 2015.

97. Tang, D., D. Wu, A. Hirao, J. M. Lahti, L. Liu, B. Mazza, V. J. Kidd, T. W. Mak and A. J. Ingram, "ERK Activation Mediates Cell Cycle Arrest and Apoptosis after DNA Damage Independently of p53", *Journal of Biological Chemistry*, Vol. 277, No. 15, pp. 12710–12717, 4 2002.

98. Ma, Q., Y. Li, Y. Fan, L. Zhao, H. Wei, C. Ji and J. Zhang, "Molecular Mechanisms of Lipoic Acid Protection against Aflatoxin B_1-Induced Liver Oxidative Damage and Inflammatory Responses in Broilers.", *Toxins*, Vol. 7, No. 12, pp. 5435–47, 12 2015.

99. Sauvant, C., H. Holzinger and M. Gekle, "Proximal Tubular Toxicity of Ochratoxin A Is Amplified by Simultaneous Inhibition of the Extracellular Signal-Regulated Kinases 1/2", *Journal of Pharmacology and Experimental Therapeutics*, Vol. 313, No. 1, pp. 234–241, 11 2004.

100. Rached, E., E. Pfeiffer, W. Dekant and A. Mally, "Ochratoxin A: Apoptosis and Aberrant Exit from Mitosis due to Perturbation of Microtubule Dynamics?", *Toxicological Sciences*, Vol. 92, No. 1, pp. 78–86, 7 2006.

101. Ramyaa, P., R. krishnaswamy and V. V. Padma, "Quercetin modulates OTA-induced oxidative stress and redox signalling in HepG2 cells — up regulation of Nrf2 expression and down regulation of NF-κB and COX-2", *Biochimica et Biophysica Acta (BBA) - General Subjects*, Vol. 1840, No. 1, pp. 681–692, 1 2014.

102. Oroojalian, F., A. H. Rezayan, W. T. Shier, K. Abnous and M. Ramezani, "Megalin-targeted enhanced transfection efficiency in cultured human HK-2 renal tubular proximal cells using aminoglycoside-carboxyalkyl- polyethylenimine -containing nanoplexes", *International Journal of Pharmaceutics*, Vol. 523, No. 1, pp. 102–120, 5 2017.

103. Wang, Y., J. Liu, J. Cui, L. Xing, J. Wang, X. Yan and X. Zhang, "ERK and p38 MAPK signaling pathways are involved in ochratoxin A-induced G2 phase arrest in human gastric epithelium cells", *Toxicology Letters*, Vol. 209, No. 2, pp. 186–192, 3 2012.

104. Jiang, B., S. Xu, X. Hou, D. R. Pimentel, P. Brecher and R. A. Cohen, "Temporal control of NF-kappaB activation by ERK differentially regulates interleukin-1beta-induced gene expression.", *The Journal of biological chemistry*, Vol. 279, No. 2, pp. 1323–9, 1 2004.

105. Faghiri, Z., C. Eiswirth and N. Bazan, "RelA (p65) NF–B Translocation and ERK Phosphorylation Modulate RPE Cell–Signal Integration During Oxidative Stress–Induced Apoptosis", *Investigative Ophthalmology & Visual Science*, Vol. 46, pp. 1601–1601, 5 2005.

106. Greene, W. C. and L.-f. Chen, "Regulation of NF-kappaB action by reversible acetylation.", *Novartis Foundation symposium*, Vol. 259, pp. 208–17, 2004.

107. Xu, H., S. Hao, F. Gan, H. Wang, J. Xu, D. Liu and K. Huang, "In vitro immune toxicity of ochratoxin A in porcine alveolar macrophages: A role for the ROS-relative TLR4/MyD88 signaling pathway", *Chemico-Biological Interactions*, Vol. 272, pp. 107–116, 6 2017.

108. van Engeland, M., L. J. Nieland, F. C. Ramaekers, B. Schutte and C. P. Reutelingsperger, "Annexin V-affinity assay: a review on an apoptosis detection system based on phosphatidylserine exposure.", *Cytometry*, Vol. 31, No. 1, pp. 1–9, 1 1998.

109. Porter, A. G. and R. U. Jänicke, "Emerging roles of caspase-3 in apoptosis", *Cell Death & Differentiation*, Vol. 6, No. 2, pp. 99–104, 2 1999.

110. Lamkanfi, M. and T.-D. Kanneganti, "Caspase-7: a protease involved in apoptosis and inflammation.", *The international journal of biochemistry & cell biology*, Vol. 42, No. 1, pp. 21–4, 1 2010.

111. Trask, O. J., *Nuclear Factor Kappa B (NF-κB) Translocation Assay Development and Validation for High Content Screening*, Eli Lilly & Company and the National Center for Advancing Translational Sciences, 10 2004.

112. Maresca, M., N. Yahi, L. Younès-Sakr, M. Boyron, B. Caporiccio and J. Fantini, "Both direct and indirect effects account for the pro-inflammatory activity of enteropathogenic mycotoxins on the human intestinal epithelium: Stimulation of interleukin-8 secretion, potentiation of interleukin-1β effect and increase in the transepithelial passage of commensal bacteria", *Toxicology and Applied Pharmacology*, Vol. 228, No. 1, pp. 84–92, 4 2008.

113. Al-Anati, L., R. Reinehr, N. Van Rooijen and E. Petzinger, "In vitro induction of tumor necrosis factor-α by ochratoxin A (OTA) from rat liver: role of Kupffer cells", *Mycotoxin Research*, Vol. 21, No. 3, pp. 172–175, 9 2005.

114. Kagoya, Y., A. Yoshimi, S. Arai, K. Kataoka, M. Nakagawa, K. Kumano and M. Kurokawa, "NF-κB/TNF-α Positive Feedback Loop with Active Proteasome Machinery Supports Myeloid Leukemia Initiating Cell Capacity", *Blood*, Vol. 120, No. 21, 2012.

115. Streicher, K. L., N. E. Willmarth, J. Garcia, J. L. Boerner, T. G. Dewey and S. P. Ethier, "Activation of a Nuclear Factor KB/Interleukin-1 Positive Feedback Loop by Amphiregulin in Human Breast Cancer Cells", *Mol Cancer Res*, Vol. 5, No. 8, pp. 847–62, 2007.